



Published in final edited form as:

J Med Chem. 2017 May 25; 60(10): 4267–4278. doi:10.1021/acs.jmedchem.7b00172.

Design and Development of Highly Potent HIV-1 Protease Inhibitors with a Crown-like Oxotricyclic Core as the P2-Ligand to Combat Multidrug-Resistant HIV Variants

Arun K. Ghosh^{*,†}, Kalapala Venkateswara Rao[†], Prasanth R. Nyalapatla[†], Heather L. Osswald[†], Cuthbert D. Martyr[†], Manabu Aoki^{‡,^,§}, Hironori Hayashi^{‡,#}, Johnson Agniswamy[‡], Yuan-Fang Wang[‡], Haydar Bulut[§], Debananda Das[§], Irene T. Weber[‡], and Hiroaki Mitsuya^{‡,#,§}

[†]Department of Chemistry and Department of Medicinal Chemistry, Purdue University, West Lafayette, IN 47907, USA

[‡]Department of Biology, Molecular Basis of Disease, Georgia State University, Atlanta, Georgia 30303, USA

[‡]Departments of Infectious Diseases and Hematology, Kumamoto University Graduate School of Biomedical Sciences, Kumamoto 860-8556, Japan

[^]Department of Medical Technology, Kumamoto Health Science University, Kumamoto 861-5598, Japan

[#]Department of Refractory Viral Infection, National Center for Global Health and Medicine Research Institute, Tokyo 162-8655, Japan

[§]Experimental Retrovirology Section, HIV and AIDS Malignancy Branch, National Cancer Institute, National Institutes of Health, Bethesda, MD 20892, USA

Abstract

Design, synthesis, and evaluation of a new class of exceptionally potent HIV-1 protease inhibitors is reported. Inhibitor **5** displayed superior antiviral activity and drug-resistance profiles. In fact, this inhibitor showed several orders of magnitude improved antiviral activity over the FDA approved drug, darunavir. This inhibitor incorporates an unprecedented 6-5-5 ring-fused crown-like tetrahydropyranofuran as the P2 ligand and an aminobenzothiazole as the P2' ligand with the (*R*)-hydroxyethylsulfonamide isostere. The crown-like P2 ligand for this inhibitor has been synthesized efficiently in an optically active form using a chiral Diels-Alder catalyst providing a key intermediate in high enantiomeric purity. Two high resolution X-ray structures of inhibitor-

*The corresponding author: Department of Chemistry and Department of Medicinal Chemistry, Purdue University, 560 Oval Drive, West Lafayette, IN 47907, Phone: (765)-494-5323; Fax: (765)-496-1612, akghosh@purdue.edu.

ASSOCIATED CONTENT

Supporting Information. The Supporting Information is available free of charge on the ACS Publication website at <http://pubs.acs.org>.

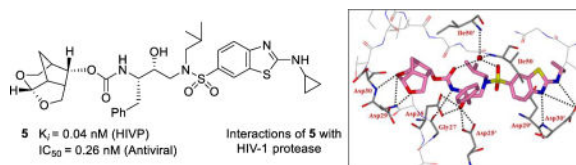
X-ray structural data for inhibitors **3b** and **4b**-bound HIV-1 Protease

Molecular formula strings and some data (CSV)

PDB ID Codes. Inhibitors **5** and **25**-bound HIV-1 protease X-ray structures are: 5TYR and 5ULT. Authors will release the atomic coordinates upon article publication.

bound HIV-1 protease revealed extensive interactions with the backbone atoms of HIV-1 protease and provided molecular insight into the binding properties of these new inhibitors.

Graphical Table of Content



Keywords

HIV-1 protease; inhibitors; antiviral; multidrug-resistant; synthesis; X-ray crystal structure; Crown-THF; backbone binding

Introduction

The introduction of protease inhibitors (PIs) in combination with antiretroviral therapies (ART) dramatically improved the treatment of patients with HIV-1 infection and AIDS.^{1,2} The ART regimens have demonstrated prolonged suppression of HIV-1 replication in treated patients. This led to marked improvements in HIV-related morbidity and mortality in developed countries.^{3,4} Despite this progress, one major issue of current PIs is that in many patients, HIV RNA levels have relapsed due to the emergence of drug-resistant HIV-1 variants, rendering a majority of current PIs ineffective within months. This has raised a significant concern for long-term treatment prognosis.^{5,6} Therefore, the design and development of new PIs with broad-spectrum antiviral activity for treatment-experienced patients remains an urgent priority.^{7,8}

Our protein-X-ray structure-based design strategies are based upon promoting extensive interactions in the active site of HIV-1 protease, particularly with the backbone atoms.^{9,10,11} We have examined and compared X-ray structural variations of critical active site interactions of numerous HIV-1 PIs bound to both wild-type and mutant proteases. These studies revealed that the backbone conformation of the active sites of various mutant proteases are only minimally distorted compared to wild-type HIV-1 protease.^{12,13} It is fundamentally very striking that a protease cannot significantly alter its overall active site backbone conformation without compromising its vital catalytic fitness for viral replication.^{9,14} Therefore, a promising inhibitor design strategy would be to maximize active site interactions and particularly to promote a robust network of hydrogen-bonding interactions with backbone atoms of wild-type HIV-1 protease. Such inhibitors will likely maintain those active site interactions with other protease mutants.^{9,11} In essence, the backbone binding strategies may lead to inhibitors that would slow development of drug-resistant HIV-1 variants due to possible reduction of catalytic fitness. HIV-1 protease in its active form is a homodimer containing catalytic aspartic acid residues in the active site. As depicted in Figure 1, our inhibitor design model to combat drug-resistance involves the design of P2 and P2' ligands that would form robust hydrogen bonds with polar groups in

S2 and S2' regions.¹⁵ Furthermore, we plan to fill in the hydrophobic S1 and S1' subsites with hydrophobic P1 and P1' ligands. Among many possible classes of transition-state binders, we plan to incorporate an (*R*)-hydroxyethylamine sulfonamide isostere, as it can be synthesized readily with varying P1 and P1' substituents to provide the nonpeptide drug-like scaffold.

Over the years, our structure-based design of a variety of P2-ligands has been based upon cyclic-ether templates where the ether oxygens are positioned to effectively mimic the carbonyl oxygens of peptide bonds. These structural templates were designed with defined stereoconfiguration and structural complementarity to effectively fill in the hydrophobic pockets in the active site. Our laboratories have designed and synthesized a range of exceptionally potent nonpeptide HIV-1 PIs showing good drug-like properties.^{16,17} One of these PIs is the FDA approved drug, darunavir (DRV, **1**, Figure 2), which was designed to promote extensive active site interactions with backbone atoms of the HIV-1 protease active site.^{18,19} DRV has emerged as the first-line therapy for rescue treatment in current US Department of Health and Human Service (DHHS) guidelines. DRV's superb resistance profile is likely due to its extensive interactions, particularly the network of hydrogen bonding interactions in the active site as evidenced by X-ray structural studies.^{9,11,20,21} The *bis*-THF ligand in DRV is an intriguing pharmacophore. Both oxygens of the *bis*-THF form very strong hydrogen bonds with Asp29 and Asp30 backbone amide NHs. Furthermore, the bicyclic ring forms nice van der Waals interactions with residues in the S2 subsite.^{22–26} To further optimize the *bis*-THF structural template, we have investigated structural templates that would enhance the backbone-binding interactions, as well as further improve van der Waals interactions within the S2 subsite of the HIV-1 protease active site. Herein, we report the design, synthesis, and X-ray structural studies of a new class of PIs incorporating an unprecedented 6-5-5 ring-fused crown-like tetrahydropyranofuran as the P2 ligand with the (*R*)-hydroxyethylsulfonamide isostere.

Results and Discussion

Our examination of the X-ray crystal structure of DRV-bound HIV-1 protease and subsequent modeling suggested that the *bis*-THF ring binding properties can be further optimized. In particular, we planned to optimize the structural template of the *bis*-THF ligand in DRV that could enhance the backbone binding as well as improve hydrophobic interactions with the protease active site. The *bis*-THF ligand in DRV and its methoxy derivative **2** (TMC-126)²³ show a distance of about 3.0 to 3.2 Å between the cyclic ether oxygens and the Asp30 backbone amide NH and a shorter and stronger hydrogen bond with the Asp29 amide NH in the X-ray structure. Based upon this ligand-binding site interactions, we subsequently designed a stereochemically defined hexahydrofurofuranol-derived urethane as the P2-ligand in inhibitor **3**. We speculated that the bicyclic acetal on a 6-5 system would have favorable alignment with backbone residues in the S2-subsite. Also, we presumed that extra methylene group on the tetrahydropyran would increase van der Waals interaction in the active site. Indeed, inhibitor **3** displayed excellent enzyme inhibitory and antiviral activity ($K_i = 2.7$ pM and $EC_{50} = 0.5$ nM). Also, this inhibitor maintained excellent potency against multidrug-resistant HIV-1 variants similar to DRV and inhibitor **2**.²⁷ To promote stronger hydrogen bonds with the top oxygen of *bis*-THF, we further hypothesized

that a larger seven-membered ring could increase the dihedral angle of the bicyclic acetal template and thereby put the top oxygen closer to the Asp30 backbone amide NH. Our preliminary model showed a more optimal alignment of Asp30 NH with the top cyclic oxygen. Since the conformation of a seven-membered ring is usually labile, we sought to incorporate a bridged methylene group on the seven-membered ring to constrain the conformational flexibility. In essence, our new design will incorporate three extra methylene groups over *bis*-THF ligand. The positions of these methylene groups may provide more favorable van der Waals interactions in the hydrophobic space surrounding Ile47, Val32, Leu76, Ile84, and Ile50' residues. We have now designed a crown-like-tetrahydropyranofuran (*crn*-THF) derivative as the novel P2-ligand shown in inhibitor **4**. A larger ring as the P2 ligand with some degree of flexibility may show better adaptability to protease mutation. Furthermore, we speculated that with new interactions in the S2-subsite, it may be necessary to optimize the P2'-sulfonamide ligand as well. To promote further hydrogen bonding interactions as well as to improve hydrophobic contacts in the S2'-subsite, we have planned to investigate inhibitors with a *crn*-THF P2-ligand in combination with a benzothiazole derivative with a small alkylamine as represented in inhibitor **5** to interact with the Asp30' residue in the S2'-subsite. In general, aminobenzothiazoles are structural features of numerous medicinally important compounds and these templates may further improve the inhibitors' drug-like properties.^{28,29}

Our synthesis of *crn*-THF P2 ligand is shown in Scheme 1. For the enantioselective synthesis of this unprecedented ligand, we planned to utilize a chiral oxazaborolidinium cation catalyzed Diels-Alder reaction developed by Corey and Mukherjee.^{30,31} The requisite oxazaborolidinium cation **6** was generated *in situ* from the corresponding oxazaborolidine (25 mol%) and triflimide (20 mol%) as reported.³⁰ The Diels-Alder reaction of readily available ethyl vinyl boronate **7**³² and cyclopentadiene at -78 °C for 7 h provided the corresponding cycloadduct which was oxidized with H₂O₂ in the presence of KHCO₃ to provide alcohol **8** in 80% yield over 2-steps in gram scale. Optical purity of alcohol **8** was determined to be 98% *ee* by chiral HPLC analysis [compound **8**, [α]_D = -141.5 (*c*1.04, CHCl₃)]. Alcohol **8** was treated with TBSOTf in the presence of 2,6-lutidine in CH₂Cl₂ at 0 °C to 23 °C for 45 min to afford TBS ether **9** in 95% yield. Ester **9** was converted to bicyclic acetal **10** in a three-step sequence involving (1) reduction of the ester with LAH in THF at 0 °C to 23 °C for 1.5 h; (2) one-pot oxidative cleavage of the olefin using Nicolaou's protocol³³; and (3) reduction of the resulting aldehyde with DIBAL-H in CH₂Cl₂ at 0 °C for 4 h. Bicyclic acetal **10** (2:1 mixture) was obtained in 62% yield over 3-steps. The lactol mixture was treated with trifluoroacetic acid (TFA) in CH₂Cl₂ at 0 °C to 23 °C for 15 h to afford bridged tricyclic derivative **11**. Removal of the TBS group with tetrabutylammonium fluoride (TBAF) in THF at 0 °C to 23 °C for 2 h provided alcohol **12** in 68% yield over 2-steps. This *exo*-alcohol was converted to *endo*-alcohol **13** by Dess-Martin oxidation at 0 °C to 23 °C for 3 h followed by reduction of the resulting ketone with NaBH₄ in MeOH at 0 °C for 45 min. The desired bridged tricyclic ligand, (3*S*, 3*a,S*, 5*R*, 7*a,S*, 8*S*)-hexahydro-4*H*-3,5-methanofuro[2,3-*b*]pyran-8-ol (**13**) was obtained in 76% yield over 2-steps. The overall route is quite efficient and provided convenient access to both *endo*- and *exo*-ligand alcohols in optically active form (>99% *ee*). Both *exo*- and *endo*-alcohols **12** and **13**, respectively, were converted to the corresponding mixed activated carbonate derivatives.^{34,35} Treatment

of these alcohols with 4-nitrophenyl chloroformate and pyridine in CH_2Cl_2 at 0 °C to 23 °C for 12 h, furnished carbonates **14** and **15** in excellent yields.

The synthesis of (*R*)-hydroxysulfonamide isostere **21** is shown in Scheme 2. Azidooxirane **17** was prepared from commercially available phenyl-2-buten-1-ol (**16**) p using Sharpless epoxidation followed by epoxide ring opening and conversion of the diol to epoxide **17**.^{36–38} Reaction of this oxirane with isobutylamine followed by treatment of the resulting amino alcohol with sulfonyl chloride **18** in CH_2Cl_2 in the presence of triethylamine at 23 °C for 12 h provided azidoalcohol **19** in excellent yields (90%) over 2-steps. Staudinger reduction³⁹ of azide **19** with Ph_3P in aqueous THF at 23 °C for 24 h followed by reaction of the resulting amine with Boc_2O afforded Boc-derivative **20** in excellent yield (85%) over 2-steps. This methylsulfide was converted to the cyclopropylamino-benzothiazole derivative **21** in a three-step sequence involving: (1) mCPBA oxidation of sulfide to sulfone at 23 °C for 12 h, (2) treatment of the resulting sulfone with cyclopropylamine in THF at 65 °C for 12 h; and (3) treatment of the resulting Boc-derivative with TFA in CH_2Cl_2 at 0 °C for 1 h. Amine **21** was obtained in excellent yield.

The synthesis of various inhibitors containing *crn*-THF as the P2 ligand is shown in Scheme 3. For the synthesis of inhibitors with 4-methoxybenzenesulfonamide as the P2'-ligand, activated carbonates of the *endo*- and *exo*-*crn*-THF **14** and **15** respectively, were reacted with known^{34,35} 4-methoxybenzenesulfonamide isostere **22** in the presence of diisopropylethylamine (DIPEA) at 23 °C for 72 h to furnish inhibitors **24** and **25** in good yields. Similarly, reaction of activated carbonate **14** with 4-aminobenzenesulfonamide isostere **23** provided inhibitor **4**. For the synthesis of inhibitors with benzothiazolesulfonamide as the P2'-ligand, known^{34,35} *bis*-THF carbonate **26** was reacted with benzothiazole derivative **21** in CH_3CN at 23 °C for 36 h to provide inhibitor **27** in good yields. Similarly, reaction of activated carbonate of *endo*-*crn*-THF **14** with benzothiazole derivative **21** provided inhibitor **5** in very good yield.

Our examination of the preliminary model of *endo*-*crn*-THF containing inhibitor **25** and *exo*-*crn*-THF-derived inhibitor **24** indicated that the acetal oxygens in the *endo*-derivative are suitably positioned to form hydrogen bonds with Asp30 and Asp29 amide NHs. Also, the tricyclic scaffold of inhibitor **25** appeared to fill the hydrophobic pocket in the S2 site more effectively than inhibitor **24**. As can be seen in Table 1, inhibitor **25** containing *endo*-*crn*-THF ligand and a 4-methoxybenzenesulfonamide as P2'-ligand, exhibited an enzyme inhibitory K_i of 14 pM compared to inhibitor **24** containing *exo*-*crn*-THF ligand (K_i of 10.8 nM). We utilized the assay protocol developed by Toth and Marshall.⁴⁰ The corresponding inhibitor **4**, with a 4-aminobenzene sulfonamide as P2'-ligand, displayed a comparable K_i value of 13 pM. We have determined antiviral activity of these inhibitors in MT-2 human T-lymphoid cells exposed to HIV_{LAI} .⁴¹ As shown, inhibitor **24** with an *exo*-*crn*-THF P2-ligand showed no appreciable antiviral activity ($\text{IC}_{50} > 1 \mu\text{M}$). However, inhibitor **25** with an *endo*-*crn*-THF displayed an antiviral IC_{50} value of 2.7 nM. Inhibitor **4**, with a DRV isostere, showed an antiviral IC_{50} value of 2.8 nM. Antiviral activity of inhibitor **27**, with a *bis*-THF as the P2-ligand and a benzothiazole as the P2'-ligand, showed a K_i value of 10 pM and an improved antiviral IC_{50} value of 1.9 nM compared to DRV. Inhibitor **5** with an *endo*-*crn* P2-

ligand showed K_i value of 40 pM and significant improvement in antiviral potency with an IC_{50} value of 0.26 nM. In comparison, darunavir and saquinavir showed IC_{50} values of 3.2 nM and 21 nM, respectively.

While current antiretroviral therapy and treatment guidelines are updated regularly with the availability of new drugs or drug-effect information, PIs continue to be a critical element of current ART regimens. PIs are widely used for the treatment of naïve and experienced HIV/AIDS patients. However, heavily-ART regimen-experienced patients tend to have drug-failure with many of the currently available PIs including darunavir.^{42,43} Therefore, design and discovery of more potent PIs showing a high genetic barrier are very important to effective long-term treatment options. Since our development of DRV, our design objectives include the design of highly potent PIs that maintain potency against a variety of existing multi-PI-resistant HIV-1 variants with better selectivity index and safety profiles. Also, it is important that the new PIs do not permit, or substantially delay, the emergence of HIV-1 variants resistant to these PIs. We therefore examined both potent *crm*-THF containing PIs (**4**, **5**) and the *bis*-THF-derived inhibitor **27** against DRV-resistant HIV-1 variants. In these assays, MT-4 cells (1×10^4) were exposed to wild-type HIV-1 and three DRV-resistant variants HIV-1_{DRV}^{R20}, HIV-1_{DRV}^{R30}, and HIV-1_{DRV}^{R51} and subjected to various concentrations of each PI. IC_{50} values were determined using p24 assay.^{41, 44} The results are shown in Table 2. PI **4** containing the *crm*-THF as the P2 ligand on the DRV-isostere, displayed comparable antiviral activity to DRV. The fold-differences in the IC_{50} value of **4** against all three DRV-resistant HIV-1 variants compared to wild-type HIV-1_{NL4-3} were similar to DRV. These DRV-resistant variants HIV-1_{DRV}^Rs are highly resistant to all current clinically used PIs including DRV and Nucleoside/Nucleotide Reverse Transcriptase Inhibitors (NRTIs) such as tenofovir.

Inhibitor **27**, containing a cyclopropylaminobenzothiazole as the P2' ligand on DRV, showed an improved antiviral activity compared to inhibitor **4** and DRV. As can be seen, the fold-differences in the IC_{50} values of **27** against HIV-1_{DRV}^{R20} and HIV-1_{DRV}^{R30} compared to wild-type HIV-1_{NL4-3} were 4- and 15-fold, respectively, while the fold-difference for DRV were 9- and 95-fold, respectively. These results indicated that the benzothiazole P2' ligand exerts a more favorable interaction in the S2' site compared to 4-aminobenzenesulfonamide of DRV. Inhibitor **5** containing *crm*-THF as the P2 ligand and aminobenzothiazole as the P2' ligand potently blocked the replication of wild-type HIV-1_{NL4-3} by a factor of 10 compared to DRV. Furthermore, this inhibitor suppressed the replication of all three DRV-resistant variants. Of particular note, the fold-differences of **5** against HIV-1_{DRV}^{R20} and HIV-1_{DRV}^{R30} compared to HIV-1_{NL4-3} were 0.4- and 5-fold, respectively. This PI also maintained IC_{50} values of 35 nM against HIV-1_{DRV}^{R51}, the most multi-PI/NRTI-resistant HIV-1 variants.

We then examined whether inhibitor **5** was active against a variety of HIV-1 variants that had been selected *in vitro* with each of seven FDA-approved PIs, SQV, APV, LPV, IDV, NFV, ATV, and TPV. Each of these HIV-1 variants were selected *in vitro* by propagating HIV-1_{NL4-3} in the presence of increasing concentrations of each PI (up to 5 μ M) in MT-4 cells.^{41, 44} They were shown to have acquired multiple amino acid substitutions in the protease of the virus that are associated with viral resistance to each PI drug. Each variant

was highly resistant to the PI, with which the variant was selected.^{41, 44} The results are shown in Table 3. As shown, two current clinically used PIs, LPV and ATV, lost significant activity against the seven HIV-1 variants. DRV showed relatively better results, however, it too failed to block replication of each variant very effectively. DRV displayed an IC₅₀ value fold-change ranging 2- to 113-fold. On the contrary, inhibitor **5** maintained superior activity against all seven HIV-1 variants showing significantly more potent antiviral activity compared to wild-type HIV_{NL4-3}. Inhibitor **5** exerted very potent antiviral activity with IC₅₀ values ranging 0.0026 to 0.27 nM. Our detailed X-ray crystallographic studies of inhibitors **5** and **25**-bound HIV-1 protease provided molecular insight into the binding properties responsible for the superior bioactivity of inhibitor **5**.

The X-ray crystal structure of the wild type HIV-1 protease co-crystallized with inhibitor **25** was refined to an R factor of 17.9% at the high resolution of 1.53 Å (PDB code : 5ULT).⁴⁵ The crystal structure contains the protease dimer and the inhibitor bound to HIV-1 protease in two orientations related by a 180° rotation with 55/45% relative occupancies. The overall structure is very similar to the structure with HIV-1 protease and DRV²¹ with root mean square difference of 0.25 Å for Cα atoms. The largest difference between corresponding Cα atoms is 0.8 Å. The inhibitor is bound in the active site cavity by forming a series of hydrogen bonding interactions and numerous weaker CH...O interactions with the main chain atoms of HIV-1 protease. As shown in Figure 3, the major conformation of the inhibitor forms hydrogen bonding interactions of its urethane NH with the carbonyl oxygen of Gly27. The inhibitor also forms tetra- coordinated water-mediated interactions connecting the inhibitor carbonyl oxygen and sulfonamide oxygen with the amides of Ile50 and Ile50' in the flaps. Furthermore, the *p*-methoxy group of the P2'-sulfonamide forms a hydrogen bond with the amide NH of Asp30' as well as with its side chain carboxyl group.

As highlighted in Figure 4, the majority of differences of inhibitor **25** and DRV are confined to the interactions of the novel *crn*-THF like tricyclic P2-ligand in inhibitor **25**, which forms a crown-like shape. The tricyclic crown scaffold is suitably substituted with two acetal oxygens to interact with backbone residues and the side chain Asp30 carboxylate group in S2 subsite. Indeed, both oxygens form hydrogen bonds with the amide groups of protease residues Asp29 and Asp30, comparable to the interactions of darunavir. The new P2-ligand is conformationally rigid and larger than the P2 *bis*-THF ligand in DRV. Our structural analysis revealed that the *crn*-THF ligand displaces residues 45'–48' by up to 0.8 Å, resulting in an enlarged inhibitor-binding cavity. The new ligand not only forms very strong hydrogen bonds with backbone atoms in the S2-site as well as with the side chain Asp29 carboxylate group. Furthermore, it also makes significantly enhanced van der Waals interactions in the S2-site compared to DRV's *bis*-THF ligand (distances of Ile47, Val32, and Leu76 are significantly shorter).

We also determined the X-ray crystal structure of inhibitor **5**-bound wild-type HIV-1 protease at a 1.7 Å resolution (PDB code: 5TYR).⁴⁴ In brief, a wild-type protease derived from wild-type HIV-1^{NL4-3} carrying no amino acid substitutions (PR^{NL4-3}) was complexed with inhibitor **5**. The inhibitor occupied the protease active site in two distinct conformations. The key inhibitor-protease interactions are shown in Figure 5. The major conformation shows that the inhibitor is bound in the active site through a network of strong

hydrogen bonds with backbone atoms as well as with catalytic aspartates. In particular, both oxygens of the *crn*-THF ligand formed strong hydrogen bonds with backbone amide NHs of Asp29 and Asp30. Furthermore, the *crn*-scaffold was involved in significant non-bonded van der Waals interactions with the HIV-1 protease. The *crn*-THF makes significantly better hydrophobic contacts than the *bis*-THF ligand in DRV. The P2' ligand's thiazole amine nitrogen also makes strong hydrogen bonds with the backbone NH of Asp30' and the cyclopropyl amine nitrogen forms additional polar interactions with the side chain carboxylate of Asp30'. This P2' ligand also makes more hydrophobic contacts with the protease than the 4-aminobenzenesulfonamide ligand of DRV. These extensive molecular interactions must be responsible for the high affinity for HIV-1 protease as well as its robust antiviral activity against multidrug-resistant HIV-1 variants. We have also compared the binding properties of the *crn*-THF ligand in the X-ray structures for inhibitors **5** and **25** to see the effect of the cyclopropylaminobenzothiazole in inhibitor **5**. As shown in Figure 6, the hydrogen bonding distance for inhibitors are nearly identical. Leu76 appears to be 0.4 Å closer to the *crn*-THF ligand in inhibitor **5**, however, Val32 shifted 0.5 Å further compared to inhibitor **25**. Overall, the binding properties of the *crn*-THF ligand in both inhibitors are very similar.

Conclusions

In summary, we investigated a new class of HIV-1 protease inhibitors by promoting ligand-backbone interactions in the active site. We designed an unprecedented crown-like hexahydrofuropranyl urethane as the P2-ligand and a cyclopropylaminobenzothiazole as the P2'-ligand with a (*R*)-hydroxysulfonamide isostere. This combination of ligands provided inhibitor **5** which displayed remarkable enzyme inhibitory and antiviral activity. Of particular importance, inhibitor **5** remained highly potent against DRV-resistant HIV-1 variants, many of which are multi-PI- and multi-NRTI-resistant HIV-1 variants. Inhibitor **5** also showed highly potent antiviral activity against a variety of HIV-1 variants selected *in vitro* with other approved PIs. These values are significantly better than other approved PIs including darunavir. Our examination of inhibitors containing *bis*-THF and aminobenzothiazole as the P2 and P2'-ligands led to very potent compound **27**. However, inhibitor **5** showed superior antiviral activity and drug-resistance profiles, several orders of magnitude improved over DRV. Furthermore, inhibitor **5** showed improved lipophilicity (clogP, 5.3) over darunavir (clogP 2.9). Our X-ray structural studies of **25**-bound and **5**-bound HIV-1 protease revealed molecular insight into the ligand-binding site interactions responsible for its exceptional drug-resistance profiles. It appears that the *crn*-THF ligand with defined configuration formed robust hydrogen bonding interactions with the backbone amide NHs of Asp29 and Asp30. Furthermore, the crown-scaffold of this new ligand is larger than the *bis*-THF of DRV and displaces residues 45' – 48' in the active site by 0.8 Å. This hydrophobic space was nicely filled by the crown-scaffold resulting in an enhanced van der Waals interaction in the S2 site. The aminobenzothiazole P2'-ligand also formed robust hydrogen bonds in the S2'-site, leading to an enhancement of ligand-binding site interactions with these combination of ligands. The *crn*-THF ligand has been synthesized efficiently in an optically active form using Corey's chiral Diels-Alder catalyst providing a key intermediate in high enantiomeric purity. The basic design of novel ligands and the

examination of ligand-combination for maximizing interactions in the enzyme active site is a powerful approach for the next generation of protease inhibitors with broad spectrum activity against multi-drug resistant HIV-1 variants.

Experimental

All moisture-sensitive reactions were carried out in oven-dried glassware under an argon atmosphere unless otherwise stated. Anhydrous solvents were obtained as follows: Diethyl ether and tetrahydrofuran were distilled from sodium metal/benzophenone under argon. Toluene and dichloromethane were distilled from calcium hydride under argon. All other solvents were reagent grade. Column chromatography was performed using Silicycle SiliaFlash F60 230–400 mesh silica gel. Thin-layer chromatography was carried out using EMD Millipore TLC silica gel 60 F₂₅₄ plates. ¹H NMR and ¹³C NMR spectra were recorded on a Varian INOVA300, Bruker ARX400, Bruker DRX500, or Bruker AV-III-500-HD. Low-resolution mass spectra were collected on a Waters 600 LCMS or by the Purdue University Campus-Wide Mass Spectrometry Center. High-resolution mass spectra were collected by the Purdue University Campus-Wide Mass Spectrometry Center. HPLC analysis and purification was done on an Agilent 1100 series instrument using a YMC Pack ODS-A column of 4.6 mm ID for analysis and either 10 mm ID or 20 mm ID for purification. The purity of all test compounds was determined by HPLC analysis to be 95% pure.

(3*S*,7*aS*,8*S*)-Hexahydro-4*H*-3,5-methanofuro[2,3-*b*]pyran-8-yl ((2*S*,3*R*)-4-((4-amino-*N*-isobutylphenyl)sulfonamido)-3-hydroxy-1-phenylbutan-2-yl)carbamate (4)

Compound **14** (18.3 mg, 0.057 mmol) was treated with isostere **23** (25 mg, 0.063 mmol) by following the procedure outlined for inhibitor **24** to give inhibitor **4** (26 mg, 80 %). ¹H NMR (500 MHz, CDCl₃) δ 7.54 (d, *J* = 8.5 Hz, 2H), 7.31 – 7.27 (m, 2H), 7.25 – 7.20 (m, 3H), 6.68 (d, *J* = 8.3 Hz, 2H), 5.42 (d, *J* = 6.6 Hz, 1H), 5.08 (d, *J* = 8.5 Hz, 1H), 4.77 (dd, *J* = 8.8, 5.8 Hz, 1H), 3.91 – 3.83 (m, 3H), 3.74 (d, *J* = 9.4 Hz, 1H), 3.59 (dd, *J* = 11.2, 8.0 Hz, 1H), 3.54 (dd, *J* = 9.2, 6.5 Hz, 1H), 3.13 (dd, *J* = 15.0, 8.4 Hz, 1H), 3.04 (dd, *J* = 14.0, 3.5 Hz, 1H), 2.99 – 2.91 (m, 2H), 2.83 (dd, *J* = 13.9, 9.1 Hz, 1H), 2.76 (dd, *J* = 13.3, 6.6 Hz, 1H), 2.72 – 2.67 (m, 1H), 2.66 – 2.62 (m, 1H), 2.37 – 2.27 (m, 1H), 1.81 (d, *J* = 11.4 Hz, 2H), 1.43 (dt, *J* = 11.8, 3.7 Hz, 1H), 0.92 (d, *J* = 6.6 Hz, 3H), 0.88 – 0.86 (m, 3H); ¹³C NMR (125 MHz, CDCl₃) δ 155.7, 150.8, 137.8, 129.6, 129.5, 128.7, 126.7, 126.3, 114.3, 104.5, 75.1, 72.8, 68.6, 60.0, 59.0, 55.2, 53.9, 45.0, 42.1, 37.5, 35.6, 31.7, 27.5, 23.6, 22.8, 20.3, 20.1, 14.3; LRMS-ESI (*m/z*): 596.4 [M+Na]⁺; HRMS-ESI (*m/z*): [M+Na]⁺ calcd for C₂₉H₃₉N₃O₇SNa, 596.2407; found 596.2402.

(3*S*,7*aS*,8*S*)-Hexahydro-4*H*-3,5-methanofuro[2,3-*b*]pyran-8-yl ((2*S*,3*R*)-4-((2-(cyclopropylamino)-*N*-isobutylbenzo[d]thiazole)-6-sulfonamido)-3-hydroxy-1-phenylbutan-2-yl)carbamate (5)

Compound **14** (14 mg, 0.044 mmol) was treated with isostere amine **21** (26 mg, 0.052 mmol) by following the procedure outlined for inhibitor **24** to give inhibitor **5** (28 mg, 97 %). ¹H NMR (500 MHz, CDCl₃) δ 8.07 (s, 1H), 7.68 (d, *J* = 8.5 Hz, 1H), 7.54 (d, *J* = 8.5 Hz, 2H), 7.29 (t, *J* = 7.4 Hz, 2H), 7.22 (dd, *J* = 13.6, 7.0 Hz, 3H), 5.41 (d, *J* = 6.7 Hz, 1H), 5.33 – 5.27 (m, 1H), 4.78 (dd, *J* = 8.7, 5.8 Hz, 1H), 3.96 – 3.84 (m, 4H), 3.73 (d, *J* = 9.3 Hz,

1H), 3.61 – 3.50 (m, 2H), 3.19 (dd, $J = 14.9, 8.3$ Hz, 1H), 3.11 – 2.96 (m, 3H), 2.84 (dt, $J = 13.4, 7.3$ Hz, 2H), 2.75 (tt, $J = 6.7, 3.5$ Hz, 1H), 2.69 (q, $J = 7.3$ Hz, 1H), 2.66 – 2.60 (m, 1H), 2.35 – 2.28 (m, 1H), 1.85 (dt, $J = 14.4, 7.0$ Hz, 1H), 1.80 (d, $J = 12.1$ Hz, 1H), 1.46 – 1.39 (m, 1H), 0.95 – 0.91 (m, 4H), 0.89 – 0.86 (m, 4H), 0.81 – 0.77 (m, 2H); ^{13}C NMR (125 MHz, CDCl_3) δ 173.3, 155.8, 137.8, 131.3, 130.4, 129.5, 128.7, 126.7, 125.5, 121.0, 118.6, 104.4, 75.1, 72.9, 68.5, 60.0, 58.9, 55.4, 53.8, 45.0, 42.1, 37.5, 35.5, 31.7, 27.4, 26.8, 23.63, 22.7, 20.3, 20.0, 14.2, 8.0; LRMS-ESI (m/z): 693.3 $[\text{M}+\text{Na}]^+$; HRMS-ESI (m/z): $[\text{M}+\text{Na}]^+$ calcd for $\text{C}_{33}\text{H}_{42}\text{N}_4\text{O}_7\text{S}_2\text{Na}$, 693.2393; found 693.2389.

Ethyl (1*S*,2*R*,3*R*,4*R*)-3-hydroxybicyclo[2.2.1]hept-5-ene-2-carboxylate (8)

To an oven and flame dried two neck round bottom flask was added a solution of oxazaborolidine (5 mL, 1.25 mmol, 0.25 M solution in toluene) and the solvent was removed under reduced pressure. The resulting residue was dissolved in 2 mL abs. CH_2Cl_2 and the clear solution was cooled to -25 °C. A solution of Tf_2NH (0.281 g in 2 mL abs. CH_2Cl_2 , 1 mmol) was added and the resulting solution was stirred at -25 °C for 25 min. Solvent was then removed carefully under reduced pressure at -25 °C. A solution of ethyl vinyl boronate **7** (1.13 g in 3 mL abs. CH_2Cl_2 , 5 mmol) was added to the resulting residue and the mixture was cooled to -78 °C. Cyclopentadiene (2.1 mL) was then added over 2 h by using syringe pump and stirred at -78 °C for another 5 h. After this period, the reaction mixture was diluted with Et_2O , warm to 23 °C and filtered through a Celite[®] pad. The filtrate was concentrated under reduced pressure and the crude product was purified by silica gel column chromatography (10 % EtOAc in hexane) to afford Diels-Alder adduct.

To a stirred solution of above Diels-Alder adduct and KHCO_3 (5 mL, 10 mmol, 2 M aqueous solution) in THF:EtOH (20 mL, 3:1) was added H_2O_2 (2 mL, 30 % wt solution in H_2O , 20 mmol) slowly at 0 °C. The resulting mixture was stirred for 4.5 h at 0 °C. Upon completion, the reaction mixture was quenched by the addition of saturated aqueous $\text{Na}_2\text{S}_2\text{O}_3$ and extracted with EtOAc. The extracts were washed with H_2O , saturated aqueous NaCl, dried (Na_2SO_4) and concentrated under reduced pressure. The crude product was purified by silica gel column chromatography (30 % EtOAc in hexane) to afford **8** (730 mg, 80 % over two steps). $[\alpha]_{\text{D}}^{20} -141.5$ (c 1.04, CHCl_3); ^1H NMR (400 MHz, CDCl_3) δ 6.13 (dd, $J = 5.7, 2.7$ Hz, 1H), 6.06 (dd, $J = 5.6, 3.3$ Hz, 1H), 4.13 – 4.04 (m, 3H), 3.07 (s, 1H), 2.77 – 2.74 (m, 1H), 2.66 (s, 1H), 2.61 (t, $J = 3.0$ Hz, 1H), 1.88 (d, $J = 8.7$ Hz, 1H), 1.63 (dd, $J = 8.7, 1.6$ Hz, 1H), 1.22 (t, $J = 7.1$ Hz, 3H); ^{13}C NMR (100 MHz, CDCl_3) δ 173.8, 137.3, 134.7, 75.7, 60.6, 55.2, 50.6, 46.4, 44.2, 14.4.

Ethyl (1*S*,2*R*,3*R*,4*R*)-3-((*tert*-butyldimethylsilyl)oxy)bicyclo[2.2.1]hept-5-ene-2-carboxylate (9)

To a stirred solution of **8** (730 mg, 4 mmol) in dichloromethane (15 mL) were added 2,6-lutidine (1.39 mL, 12 mmol) and TBSOTf (1.38 mL, 6 mmol) at 0 °C under argon atmosphere. The reaction mixture was warmed to 23 °C and stirred for 1 h. Upon completion, the reaction mixture was quenched by the addition of saturated aqueous NaHCO_3 and extracted with dichloromethane. The extracts were washed with saturated aqueous NaCl, dried (Na_2SO_4) and concentrated under reduced pressure. The crude product was purified by silica gel column chromatography (5 % Et_2O in hexane) to afford **9** (1.13 g,

95 %). ^1H NMR (400 MHz, CDCl_3) δ 6.13 (dd, $J = 5.7, 2.7$ Hz, 1H), 6.04 (dd, $J = 5.6, 3.2$ Hz, 1H), 4.13-4.04 (m, 2H), 4.03 (q, $J = 2.4, 1.5$ Hz, 1H), 3.03 (s, 1H), 2.68 – 2.62 (m, 1H), 2.57 (dd, $J = 3.5, 2.3$ Hz, 1H), 1.90 (d, $J = 8.5$ Hz, 1H), 1.60 (dq, $J = 8.4, 1.6$ Hz, 1H), 1.23 (t, $J = 7.1$ Hz, 3H), 0.88 (s, 9H), 0.07 (d, $J = 3.8$ Hz, 6H); ^{13}C NMR (100 MHz, CDCl_3) δ 173.9, 137.5, 134.6, 76.0, 60.3, 55.5, 51.4, 46.7, 44.2, 25.9, 18.1, 14.4, –4.7; LRMS-ESI (m/z): 319.1 $[\text{M}+\text{Na}]^+$.

***Tert*-butyl(((3*S*,7*aS*,8*R*)-hexahydro-4*H*-3,5-methanofuro[2,3-*b*]pyran-8-yl)oxy)dimethylsilane (11)**

To a stirred solution of ester **9** (1.13 g, 3.8 mmol) in THF (15 mL) was added LAH (360 mg, 9.5 mmol) at 0 °C under argon atmosphere. The reaction mixture was warmed to 23 °C and stirred for 1 h. Upon completion, the reaction mixture was quenched slowly by the addition of 3N NaOH solution it forms white suspension. The suspension was filtered and washed with EtOAc. The solvent was removed under reduced pressure and proceeds to the next step without further purification.

To the above crude in acetone:water (10:1, 35.2 mL) were added 2,6-lutidine (0.88 mL, 7.6 mmol), NMO (670 mg, 5.7 mmol) and OsO_4 (0.48 mL, 4 % in H_2O , 0.076 mmol) at 23 °C. The reaction mixture was stirred for 24 h as monitor by TLC and then $\text{PhI}(\text{OAc})_2$ (1.84 g, 5.7 mmol) was added. After stirring for 15h, the reaction mixture was quenched by the addition of saturated aqueous $\text{Na}_2\text{S}_2\text{O}_3$ and extracted with EtOAc. The extracts were washed with saturated aqueous CuSO_4 , H_2O , saturated aqueous NaCl, dried (Na_2SO_4) and concentrated under reduced pressure. The crude product was purified by silica gel column chromatography (25 % EtOAc in hexane) to afford the mixture of aldehydes (980 mg).

To a stirred solution of above aldehydes (980 mg, 3.42 mmol) in dichloromethane (15 mL) at 0 °C was added DIBAL-H (7.2 mL, 7.2 mmol) under argon atmosphere and stirred at the same temperature for 4 h. After this period, the reaction mixture was quenched by the addition of Saturated aqueous solution of sodium potassium tartarate and stirred vigorously at 23 °C for 2 h until two layers become clear. Organic layer was separated and aqueous layers was extracted with dichloromethane. Combined extracts were washed with saturated aqueous NaCl, dried (Na_2SO_4) and concentrated under reduced pressure. The crude product was purified by silica gel column chromatography (60 % EtOAc in hexane) to afford **10** in 2:1 ratio (670 mg, 62 % for 3 steps).

To a stirred solution of **10** (670 mg, 2.32 mmol) in dichloromethane (60 mL) was added TFA (2.3 mL) at 0 °C under argon atmosphere. The reaction mixture was warmed to 23 °C and stirred for 15 h. Upon completion, the reaction mixture was quenched by the addition of saturated aqueous NaHCO_3 and extracted with dichloromethane. The extracts were washed with saturated aqueous NaCl, dried (Na_2SO_4) and concentrated under reduced pressure. The crude product was purified by silica gel column chromatography (5 % EtOAc in hexane) to afford **11** (465 mg, 74 %). ^1H NMR (400 MHz, CDCl_3) δ 5.36 (d, $J = 6.8$ Hz, 1H), 4.11 (dd, $J = 9.0, 1.2$ Hz, 1H), 3.97 (dd, $J = 8.9, 7.0$ Hz, 1H), 3.87 – 3.79 (m, 2H), 3.51 (d, $J = 11.5$ Hz, 1H), 2.70 (q, $J = 5.9$ Hz, 1H), 2.42 (t, $J = 7.1$ Hz, 1H), 2.06 – 2.01 (m, 1H), 1.97 (dt, $J = 11.1, 4.4$ Hz, 1H), 1.83 (d, $J = 11.3$ Hz, 1H), 0.86 (s, 9H), 0.04 (d, $J = 3.8$ Hz, 6H); ^{13}C

NMR (100 MHz, CDCl₃) δ 104.2, 86.3, 73.3, 64.9, 52.7, 45.5, 44.6, 25.9, 25.6, 18.1, -4.6; LRMS-ESI (m/z): 293.1 [M+Na]⁺.

(3S,7aS,8R)-Hexahydro-4H-3,5-methanofuro[2,3-b]pyran-8-ol (12)

To a stirred solution of **11** (460 mg, 1.7 mmol) in THF (10 mL) was added TBAF (2.6 mL, 2.6 mmol) at 0 °C under argon atmosphere. The reaction mixture was warmed to 23 °C and stirred for 2 h. Upon completion, solvent was removed under reduced pressure. The crude product was purified by silica gel column chromatography (85 % EtOAc in hexane) to afford **12** (248 mg, 92 %). [α]_D²⁰ -24.48 (*c* 1.0, CHCl₃); ¹H NMR (400 MHz, CDCl₃) δ 5.39 (d, *J* = 6.8 Hz, 1H), 4.17 (dd, *J* = 9.0, 1.1 Hz, 1H), 3.99 (dd, *J* = 9.0, 6.9 Hz, 1H), 3.95 (s, 1H), 3.86 (dd, *J* = 11.5, 8.5 Hz, 1H), 3.56 (d, *J* = 11.5 Hz, 1H), 2.75 (q, *J* = 5.8 Hz, 1H), 2.47 (t, *J* = 7.0 Hz, 1H), 2.15 – 2.09 (m, 1H), 1.99 (dt, *J* = 11.6, 4.3 Hz, 1H), 1.91 (d, *J* = 11.7 Hz, 1H), 1.72 (s, 1H); ¹³C NMR (100 MHz, CDCl₃) δ 104.1, 85.7, 73.3, 64.7, 51.8, 45.5, 44.5, 25.5; LRMS-ESI (m/z): 179.0 [M+Na]⁺.

(3S,7aS,8S)-Hexahydro-4H-3,5-methanofuro[2,3-b]pyran-8-ol (13)

To a stirred solution of **12** (100 mg, 0.64 mmol) in dichloromethane (4 mL) were added Na₂HPO₄ (50 mg, 0.35 mmol) and DMP (352 mg, 0.83 mmol) at 0 °C under argon atmosphere. The reaction mixture was warmed to 23 °C and stirred for 3 h. Upon completion, the reaction mixture was quenched by the addition of saturated aqueous Na₂S₂O₃ and extracted with dichloromethane. The extracts were washed with saturated aqueous NaHCO₃, saturated aqueous NaCl, dried (Na₂SO₄) and concentrated under reduced pressure. The crude product was purified by silica gel column chromatography (40 % EtOAc in hexane) to afford ketone (88 mg, 89 %). ¹H NMR (400 MHz, CDCl₃) δ 5.57 (d, *J* = 7.0 Hz, 1H), 4.21 (d, *J* = 8.7 Hz, 1H), 3.83 – 3.76 (m, 2H), 3.68 (d, *J* = 11.2 Hz, 1H), 3.04 – 2.96 (m, 1H), 2.56 (t, *J* = 6.8 Hz, 1H), 2.39 – 2.32 (m, 1H), 2.09 (d, *J* = 12.0 Hz, 1H), 1.96 – 1.87 (m, 1H); ¹³C NMR (100 MHz, CDCl₃) δ 220.8, 104.1, 71.8, 63.3, 49.6, 46.6, 42.8, 23.3; LRMS-ESI (m/z): 177.1 [M+Na]⁺.

To a stirred solution of above ketone (87.9 mg, 0.57 mmol) in MeOH (4 mL) was added NaBH₄ (108 mg, 2.85 mmol) at 0 °C and stirred at the same temperature for 1 h. Upon completion, the reaction mixture was quenched by the addition of saturated aqueous NH₄Cl and extracted with EtOAc. The extracts were washed with saturated aqueous NaCl, dried (Na₂SO₄) and concentrated under reduced pressure. The crude product was purified by silica gel column chromatography (65 % EtOAc in hexane) to afford **13** (76 mg, 85 %). [α]_D²⁰ -9.27 (*c* 1.03, CHCl₃); ¹H NMR (400 MHz, CDCl₃) δ 5.43 (d, *J* = 6.4 Hz, 1H), 4.42 (d, *J* = 9.4 Hz, 1H), 4.23 (dd, *J* = 8.8, 5.7 Hz, 1H), 4.06 (d, *J* = 11.4 Hz, 1H), 3.74 (dd, *J* = 9.0, 6.2 Hz, 1H), 3.64 (dd, *J* = 11.4, 7.8 Hz, 1H), 2.70 – 2.58 (m, 2H), 2.23 (q, *J* = 5.5 Hz, 1H), 1.98 (s, 1H), 1.80 (d, *J* = 12.0 Hz, 1H), 1.44 (dt, *J* = 12.0, 3.9 Hz, 1H); ¹³C NMR (100 MHz, CDCl₃) δ 104.4, 72.5, 68.2, 59.4, 45.3, 43.0, 39.4, 23.9; LRMS-ESI (m/z): 179.0 [M+Na]⁺; HRMS-ESI (m/z): [M+Na]⁺ calcd for C₈H₁₂O₃Na, 179.0684; found 179.0680.

(3S,7aS,8S)-Hexahydro-4H-3,5-methanofuro[2,3-b]pyran-8-yl (4-nitrophenyl) carbonate (14)

To a stirred solution of **13** (75.6 mg, 0.484 mmol) in dichloromethane (4 mL) were added pyridine (0.18 mL, 2.2 mmol) and 4-nitrophenyl chloroformate (292 mg, 1.45 mmol) at 0 °C

under argon atmosphere. The reaction mixture was warmed to 23 °C and stirred for 12 h. Upon completion, solvent was removed under reduced pressure. The crude product was purified by silica gel column chromatography (35 % EtOAc in hexane) to afford **14** (147 mg, 94%). ¹H NMR (400 MHz, CDCl₃) δ 8.32 – 8.26 (m, 2H), 7.41 – 7.36 (m, 2H), 5.52 (d, *J* = 6.8 Hz, 1H), 5.02 (dd, *J* = 9.2, 5.7 Hz, 1H), 4.28 (d, *J* = 9.5 Hz, 1H), 4.05 (d, *J* = 11.6 Hz, 1H), 3.86 (dd, *J* = 9.5, 6.6 Hz, 1H), 3.74 (dd, *J* = 11.6, 7.9 Hz, 1H), 2.96 (q, *J* = 7.1 Hz, 1H), 2.79 (q, *J* = 6.8 Hz, 1H), 2.59 (q, *J* = 5.5 Hz, 1H), 1.95 (d, *J* = 12.2 Hz, 1H), 1.56 (dt, *J* = 12.2, 4.2 Hz, 1H); ¹³C NMR (100 MHz, CDCl₃) δ 155.5, 152.1, 145.6, 125.5, 121.8, 104.5, 79.9, 68.5, 59.7, 45.1, 42.0, 37.5, 23.7; LRMS-ESI (*m/z*): 343.9 [M+Na]⁺.

(3*S*,7*aS*,8*R*)-Hexahydro-4*H*-3,5-methanofuro[2,3-*b*]pyran-8-yl (4-nitrocyclohexa-1,5-dien-1-yl) carbonate (15)

Alcohol **12** (9.5 mg, 0.061 mmol) was treated with 4-nitrophenyl chloroformate (24.6 mg, 0.122 mmol) by following the procedure above to afford **15** (17.5 mg, 90%). ¹H NMR (400 MHz, CDCl₃) δ 8.31 – 8.26 (m, 2H), 7.41 – 7.35 (m, 2H), 5.45 (d, *J* = 6.7 Hz, 1H), 4.78 (s, 1H), 4.28 (d, *J* = 9.3 Hz, 1H), 4.03 (dd, *J* = 9.3, 6.6 Hz, 1H), 3.95 (dd, *J* = 11.7, 8.6 Hz, 1H), 3.66 (d, *J* = 11.7 Hz, 1H), 2.88 – 2.81 (m, 1H), 2.73 (t, *J* = 6.8 Hz, 1H), 2.49 – 2.43 (m, 1H), 2.05 – 1.95 (m, 2H); ¹³C NMR (100 MHz, CDCl₃) δ 155.5, 152.2, 145.6, 125.5, 121.8, 104.0, 92.4, 72.8, 64.0, 49.7, 45.3, 41.4, 26.1.

***N*-((2*R*,3*S*)-3-Amino-2-hydroxy-4-phenylbutyl)-2-(cyclopropylamino)-*N*-isobutylbenzo[*d*]thiazole-6-sulfonamide (21)**

To a stirred solution of **20** (360 mg, 0.62 mmol) in dichloromethane (5 mL) was added mCPBA (321 mg, 1.86 mmol) at 0 °C under argon atmosphere and the mixture was stirred at 23 °C for 12 h. After this period, the reaction mixture was quenched by the addition of Saturated aqueous Na₂S₂O₃ (1 mL) and extracted with dichloromethane. The extracts were washed with saturated aqueous NaHCO₃, dried (Na₂SO₄) and concentrated under reduced pressure. To the crude product in dry THF (3 mL) at 23 °C under argon atmosphere was added cyclopropylamine (0.13 mL, 1.86 mmol) and the mixture was stirred at 65 °C for 12 h. After this period, solvent was removed under reduced pressure and the crude product was purified by silica gel column chromatography (35 % EtOAc in hexane) to give Boc-derivative (334 mg, 91 % over two steps).

To a stirred solution of above Boc-derivative (334 mg, 0.57 mmol) in dichloromethane (5 mL) was added TFA (1 mL) at 0 °C under argon atmosphere and the mixture was stirred at 23 °C for 1 h. After this period, solvent was removed under reduced pressure. The crude was washed with saturated aqueous NaHCO₃, dried (Na₂SO₄) and concentrated under reduced pressure. The crude product was purified by silica gel column chromatography (5 % MeOH in CH₂Cl₂) to afford **21** (275 mg, 99 % yield). ¹H NMR (500 MHz, CDCl₃) δ 8.11 (d, *J* = 1.5 Hz, 1H), 7.71 (dd, *J* = 8.5, 1.6 Hz, 1H), 7.49 (d, *J* = 8.5 Hz, 1H), 7.31 (t, *J* = 7.4 Hz, 2H), 7.22 (dd, *J* = 12.5, 7.1 Hz, 3H), 3.85 – 3.78 (m, 1H), 3.31 (d, *J* = 7.4 Hz, 2H), 3.19 – 3.11 (m, 1H), 3.07 (dd, *J* = 13.3, 8.3 Hz, 1H), 3.01 – 2.87 (m, 2H), 2.73 (tt, *J* = 6.7, 3.5 Hz, 1H), 2.56 – 2.46 (m, 1H), 1.96 – 1.85 (m, 1H), 0.95 – 0.92 (m, 4H), 0.90 – 0.88 (m, 4H), 0.79 – 0.76 (m, 2H); ¹³C NMR (125 MHz, CDCl₃) δ 173.1, 155.6, 138.9, 131.2, 131.0, 129.4, 128.8, 126.6, 125.5, 121.0, 118.6, 73.1, 58.7, 55.8, 52.7, 39.1, 31.7, 27.3, 26.8, 22.8, 20.4,

20.1, 14.3, 8.0; LRMS-ESI (m/z): 489.2 [M]⁺, 490.2 [M+H]⁺; HRMS-ESI (m/z): [M+H]⁺ calcd for C₂₄H₃₃N₄O₃S₂, 489.1994; found 489.1986.

(3S,7aS,8R)-Hexahydro-4H-3,5-methanofuro[2,3-b]pyran-8-yl ((2S,3R)-3-hydroxy-4-((N-isobutyl-4-methoxyphenyl)sulfonamido)-1-phenylbutan-2-yl)carbamate (24)

To a stirred solution of activated alcohol **15** (17.3 mg, 0.054 mmol) and isostere **22** (24 mg, 0.059 mmol) in acetonitrile (2 mL) was added DIPEA (42 μ L, 0.24 mmol) at 23 °C under argon atmosphere. The reaction mixture was stirred at 23 °C until completion. Upon completion, solvents were removed under reduced pressure and crude product was purified by silica gel column chromatography (45 % EtOAc in hexane) to give inhibitor **24** (26.4 mg, 83 %). ¹H NMR (400 MHz, CDCl₃) δ 7.69 (d, J = 8.7 Hz, 2H), 7.30 – 7.26 (m, 2H), 7.23 – 7.20 (m, 3H), 6.97 (d, J = 8.8 Hz, 2H), 5.38 (d, J = 6.6 Hz, 1H), 4.88 (d, J = 8.1 Hz, 1H), 4.50 (s, 1H), 4.19 (d, J = 9.0 Hz, 1H), 4.00 – 3.91 (m, 1H), 3.88 – 3.78 (m, 7H), 3.54 (d, J = 11.6 Hz, 1H), 3.12 (dd, J = 15.1, 8.2 Hz, 1H), 3.05 – 2.96 (m, 2H), 2.97 – 2.92 (m, 1H), 2.89 – 2.83 (m, 1H), 2.78 (dd, J = 13.4, 6.7 Hz, 1H), 2.69 (s, 1H), 2.46 (t, J = 6.0 Hz, 1H), 2.02 (s, 1H), 1.86 – 1.80 (m, 2H), 1.75 – 1.70 (m, 1H), 0.91 (d, J = 6.6 Hz, 3H), 0.86 (d, J = 6.5 Hz, 3H); ¹³C NMR (100 MHz, CDCl₃) δ 163.2, 156.0, 137.8, 129.9, 129.6, 128.6, 126.6, 114.5, 104.0, 88.0, 73.0, 72.8, 64.4, 58.9, 55.8, 55.1, 53.8, 49.4, 45.2, 41.3, 35.6, 27.4, 25.9, 20.3, 20.0; LRMS-ESI (m/z): 611.4 [M+Na]⁺; HRMS-ESI (m/z): [M+Na]⁺ calcd for C₃₀H₄₀N₂O₈SNa, 611.2404; found 611.2408.

(3S,7aS,8S)-Hexahydro-4H-3,5-methanofuro[2,3-b]pyran-8-yl ((2S,3R)-3-hydroxy-4-((N-isobutyl-4-methoxyphenyl)sulfonamido)-1-phenylbutan-2-yl)carbamate (25)

Compound **14** (21.2 mg, 0.066 mmol) was treated with isostere **22** (29.7 mg, 0.073 mmol) by following the procedure above to afford inhibitor **25** (34.5 mg, 89 %). ¹H NMR (400 MHz, CDCl₃) δ 7.71 (d, J = 8.8 Hz, 2H), 7.32 – 7.26 (m, 2H), 7.25 – 7.20 (m, 3H), 6.97 (d, J = 8.8 Hz, 2H), 5.41 (d, J = 6.6 Hz, 1H), 5.14 (d, J = 8.5 Hz, 1H), 4.78 (dd, J = 8.6, 5.8 Hz, 1H), 3.92 – 3.80 (m, 7H), 3.74 (d, J = 9.1 Hz, 1H), 3.56 (ddd, J = 16.0, 10.2, 7.2 Hz, 2H), 3.14 (dd, J = 15.0, 8.2 Hz, 1H), 3.05 (dd, J = 14.2, 3.6 Hz, 1H), 3.02 – 2.92 (m, 2H), 2.81 (td, J = 14.9, 13.4, 7.7 Hz, 2H), 2.66 (td, J = 13.4, 10.7, 7.1 Hz, 2H), 2.35 – 2.27 (m, 1H), 1.83 (dd, J = 20.5, 9.2 Hz, 2H), 1.43 (dt, J = 11.9, 4.2 Hz, 1H), 0.91 (d, J = 6.6 Hz, 3H), 0.87 (d, J = 6.9 Hz, 3H); ¹³C NMR (100 MHz, CDCl₃) δ 163.2, 155.8, 137.8, 130.0, 129.6, 129.5, 128.7, 126.7, 114.5, 104.5, 75.1, 72.9, 68.6, 60.0, 58.9, 55.8, 55.3, 53.8, 45.0, 42.1, 37.5, 35.6, 31.7, 27.4, 23.6, 22.8, 20.3, 20.0; LRMS-ESI (m/z): 611.4 [M+Na]⁺; HRMS-ESI (m/z): [M+Na]⁺ calcd for C₃₀H₄₀N₂O₈SNa, 611.2404; found 611.2401.

(3R,3aS,6aR)-Hexahydrofuro[2,3-b]furan-3-yl ((2S,3R)-4-((2-(cyclopropylamino)-N-isobutylbenzo[d]thiazole)-6-sulfonamido)-3-hydroxy-1-phenylbutan-2-yl)carbamate (27)

Compound **26** (8 mg) was treated with isostere amine **21** by following the procedure outlined for inhibitor **24** to give inhibitor **27** (15 mg, 79 %). ¹H NMR (500 MHz, CDCl₃) δ 8.12 – 8.08 (m, 1H), 7.71 (dd, J = 8.5, 1.7 Hz, 1H), 7.61 (d, J = 8.5 Hz, 1H), 7.33 – 7.29 (m, 3H), 7.27 – 7.21 (m, 3H), 6.64 (s, 1H), 5.67 (d, J = 5.1 Hz, 1H), 5.04 (dt, J = 23.9, 7.5 Hz, 2H), 4.02 – 3.95 (m, 1H), 3.95 – 3.90 (m, 2H), 3.90 – 3.85 (m, 1H), 3.77 – 3.67 (m, 3H), 3.24 (dd, J = 14.8, 8.4 Hz, 1H), 3.16 – 3.09 (m, 1H), 3.05 (dt, J = 14.7, 7.4 Hz, 2H), 2.97 –

2.90 (m, 1H), 2.86 (dd, $J = 13.3, 6.5$ Hz, 2H), 2.80 (tt, $J = 6.7, 3.5$ Hz, 1H), 1.87 (dq, $J = 13.3, 6.6$ Hz, 1H), 1.71 – 1.64 (m, 1H), 1.52 (d, $J = 9.8$ Hz, 1H), 1.01 – 0.96 (m, 5H), 0.92 (d, $J = 6.6$ Hz, 3H), 0.85 – 0.81 (m, 2H); ^{13}C NMR (125 MHz, CDCl_3) δ 173.3, 155.8, 155.6, 137.8, 131.4, 130.4, 129.5, 128.7, 126.7, 125.5, 121.0, 118.7, 109.4, 73.6, 73.0, 70.9, 69.8, 59.1, 55.3, 53.9, 45.5, 35.8, 29.8, 27.5, 26.8, 25.9, 20.3, 20.0, 8.1; LRMS-ESI (m/z): 667.4 $[\text{M}+\text{Na}]^+$; HRMS-ESI (m/z): $[\text{M}+\text{H}]^+$ calcd for $\text{C}_{31}\text{H}_{41}\text{N}_4\text{O}_7\text{S}_2$, 645.2417; found 645.2423.

Supplementary Material

Refer to Web version on PubMed Central for supplementary material.

Acknowledgments

This research was supported by the National Institutes of Health (Grant GM53386, AKG and Grant GM 62920, IW). X-ray data were collected at the Southeast Regional Collaborative Access Team (SER-CAT) beamline 22BM at the Advanced Photon Source, Argonne National Laboratory. Use of the Advanced Photon Source was supported by the US Department of Energy, Basic Energy Sciences, Office of Science, under Contract No. W-31-109-Eng-38. This work was also supported by the Intramural Research Program of the Center for Cancer Research, National Cancer Institute, National Institutes of Health, and in part by a Grant-in-Aid for Scientific Research (Priority Areas) from the Ministry of Education, Culture, Sports, Science, and Technology of Japan (Monbu Kagakusho), a Grant for Promotion of AIDS Research from the Ministry of Health, Welfare, and Labor of Japan, and the Grant to the Cooperative Research Project on Clinical and Epidemiological Studies of Emerging and Reemerging Infectious Diseases (Renkei Jigyo) of Monbu-Kagakusho. The authors would like to thank the Purdue University Center for Cancer Research, which supports the shared NMR and mass spectrometry facilities. We thank Dr. Margherita Brindisi (Purdue University) for helpful discussion.

ABBREVIATIONS USED

THF	tetrahydrofuran
bis-THF	bis-tetrahydrofuran
PI	protease inhibitor
crn-THF	<i>crown</i> -tetrahydrofuran
TFA	trifluoroacetic acid
DRV	darunavir
APV	amprenavir
NRTIs	Nucleotide Reverse Transcriptase Inhibitors
LPV	lopinavir
ATV	atazanavir

References

1. Ghosh AK, Osswald HL, Prato G. Recent Progress in the Development of HIV-1 Protease Inhibitors for the Treatment of HIV/AIDS. *J. Med. Chem.* 2016; 59:5172–5208. [PubMed: 26799988]
2. Edmonds A, Yotebieng M, Lusiana J, Matumona Y, Kitetele F, Napravnik S, Cole SR, Van Rie A, Behets F. The Effect of Highly Active Antiretroviral Therapy on the Survival of HIV-Infected

- Children in a Resource-Deprived Setting: a Cohort Study. *PLoS Med.* 2011; 8:e1001044. [PubMed: 21695087]
3. Montaner JSG, Lima VD, Barrios R, Yip B, Wood E, Kerr T, Shannon K, Harrigan PR, Hogg RS, Daly P, Kendall P. Association of Highly Active Antiretroviral Therapy Coverage, Population Viral Load, and Yearly New HIV Diagnoses in British Columbia, Canada: a Population-Based Study. *Lancet.* 2010; 376:532–539. [PubMed: 20638713]
 4. Lohse N, Hansen AB, Gerstoft J, Obel N. Improved Survival in HIV-Infected Persons: Consequences and Perspectives. *J. Antimicrob. Chemother.* 2007; 60:461–463. [PubMed: 17609196]
 5. Hue S, Gifford RJ, Dunn D, Fernhill E, Pillay D. Demonstration of Sustained Drug-Resistant Human Immunodeficiency Virus Type 1 Lineages Circulating Among Treatment-Naïve Individuals. *J. Virol.* 2009; 83:2645–2654. [PubMed: 19158238]
 6. Guidelines for the Use of Antiretroviral Agents in HIV-1-Infected Adults and Adolescents. Jul 14, 2016 <https://aidsinfo.nih.gov/contentfiles/lvguidelines/adultandadolescentgl.pdf>
 7. Saylor D, Dickens AM, Sacktor N, Haughey N, Slusher B, Pletnikov M, Mankowski JL, Brown A, Volsky DJ, McArthur JC. HIV-Associated Neurocognitive Disorder — Pathogenesis and Prospects for Treatment. *Nat. Rev. Neurol.* 2016; 12:234–248. [PubMed: 26965674]
 8. Esté JA, Cihlar T. Current Status and Challenges of Antiretroviral Research and Therapy. *Antiviral. Res.* 2010; 85:25–33. [PubMed: 20018390]
 9. Ghosh AK, Anderson DD, Weber IT, Mitsuya H. Enhancing Protein Backbone Binding—a Fruitful Concept for Combating Drug-Resistant HIV. *Angew. Chem., Int. Ed.* 2012; 51:1778–1802.
 10. Ghosh, AK., Chapsal, BD., Mitsuya, H. Darunavir, a New PI with Dual Mechanism: From a Novel Drug Design Concept to New Hope Against Drug-Resistant HIV. In: Ghosh, AK., editor. *Aspartic Acid Proteases as Therapeutic Targets, Methods and Principles in Medicinal Chemistry.* Vol. 45. Wiley-VCH; Weinheim, Germany: 2010. p. 205-243.
 11. Ghosh AK, Chapsal BD, Weber IT, Mitsuya H. Design of HIV Protease Inhibitors Targeting Protein Backbone: An Effective Strategy for Combating Drug Resistance. *Acc. Chem. Res.* 2008; 41:78–86. [PubMed: 17722874]
 12. Ghosh AK, Sridhar PR, Leshchenko S, Hussain AK, Li J, Kovalevsky AY, Walters DE, Wedekind J, Grum-Tokars V, Das D, Koh Y, Maeda K, Gatanaga H, Weber IT, Mitsuya H. Structure-Based Design of Novel HIV-1 Protease Inhibitors to Combat Drug Resistance. *J. Med. Chem.* 2006; 49:5252–5261. [PubMed: 16913714]
 13. Laco GS, Schalk-Hihi C, Lubkowski J, Morris G, Zdanov A, Olson A, Elder JH, Wlodawer A, Gustchina A. Crystal Structures of the Inactive D30N Mutant of Feline Immunodeficiency Virus Protease Complexed with a Substrate and an Inhibitor. *Biochemistry.* 1997; 36:10696–10708. [PubMed: 9271500]
 14. Agniswamy J, Weber IT. HIV-1 Protease: Structural Perspectives on Drug Resistance. *Viruses.* 2009; 1:1110–1136. [PubMed: 21994585]
 15. Ghosh, AK., Gemma, S. *Structure-Based Design of Drugs and Other Bioactive Molecules: Tools and Strategies.* Wiley-VCH; Weinheim, Germany: 2014. Development of Direct Thrombin Inhibitor, Dabigatran Etexilate, as an Anticoagulant Drug; p. 337-354.
 16. Ghosh AK, Sridhar PR, Kumaragurubaran N, Koh Y, Weber IT, Mitsuya H. Bis-Tetrahydrofuran: a Privileged Ligand for Darunavir and a New Generation of HIV Protease Inhibitors That Combat Drug Resistance. *ChemMedChem.* 2006; 1:939–950. [PubMed: 16927344]
 17. Ghosh AK, Kincaid JF, Cho W, Walters DE, Krishnan K, Hussain KA, Koo Y, Cho H, Rudall C, Holland L, Buthod J. Potent HIV Protease Inhibitors Incorporating High-Affinity P2-Ligands and (*R*)-(Hydroxyethylamino)sulfonamide Isostere. *Bioorg. Med. Chem. Lett.* 1998; 8:687–690. [PubMed: 9871583]
 18. Ghosh AK, Dawson ZL, Mitsuya H. Darunavir, a Conceptually New HIV-1 Protease Inhibitor for the Treatment of Drug-Resistant HIV. *Bioorg. Med. Chem.* 2007; 15:7576–7580. [PubMed: 17900913]
 19. Ghosh, AK., Chapsal, BD. Design of the Anti-HIV-1 Protease Inhibitor Darunavir. In: Ganellin, CR, Jefferis, R., Roberts, S., editors. *Introduction to Biological and Small Molecule Drug Research and Development: Theory and case studies.* Elsevier; London: 2013. p. 355-384.

20. Koh Y, Nakata H, Maeda K, Ogata H, Bilcer G, Devasamundram T, Kincaid JF, Boross P, Wang YF, Tie Y, Volarath P, Gaddis L, Harrison RW, Weber IT, Ghosh AK, Mitsuya H. Novel *bis*-Tetrahydrofuranyurethane-Containing Nonpeptidic Protease Inhibitor (PI) UIC-94017 (TMC114) with Potent Activity against Multi-PI-Resistant Human Immunodeficiency Virus In Vitro. *Antimicrob. Agents Chemother.* 2003; 47:3123–3129. [PubMed: 14506019]
21. Tie Y, Boross PI, Wang Y-F, Gaddis L, Hussain AK, Leshchenko S, Ghosh AK, Louis JM, Harrison RW, Weber IT. High Resolution Crystal Structures of HIV-1 Protease with a Potent Non-peptide Inhibitor (UIC-94017) Active Against Multidrug-Resistant Clinical Strains. *J. Mol. Biol.* 2004; 338:341–352. [PubMed: 15066436]
22. King NM, Prabu-Jeyabalan M, Nalivaika EA, Wigerinck P, de Bethune MP, Schiffer CA. Structural and Thermodynamic Basis for the Binding of TMC114, a Next-Generation Human Immunodeficiency Virus Type 1 Protease Inhibitor. *J. Virol.* 2004; 78:12012–12021. [PubMed: 15479840]
23. Yoshimura K, Kato R, Kavlick MF, Nguyen A, Maroun V, Maeda K, Hussain KA, Ghosh AK, Gulnik SV, Erickson JW, Mitsuya H. A Potent Human Immunodeficiency Virus Type 1 Protease Inhibitor, UIC-94003 (TMC-126), and Selection of a Novel (A28S) Mutation in the Protease Active Site. *J. Virol.* 2002; 76:1349–1358. [PubMed: 11773409]
24. De Meyer S, Azijn H, Surleraux D, Jochmans D, Tahri A, Pauwels R, Wigerinck P, de Béthune MP. TMC114, a Novel Human Immunodeficiency Virus Type 1 Protease Inhibitor Active Against Protease Inhibitor-Resistant Viruses, Including a Broad Range of Clinical Isolates. *Antimicrob. Agents Chemother.* 2005; 49:2314–2321. [PubMed: 15917527]
25. de Béthune, MP., Sekar, V., Spinosá-Guzman, S., Vanstockem, M., De Meyer, S., Wigerinck, P., Lefebvre, E. Darunavir (Prezista, TMC114): From Bench to Clinic, Improving Treatment Options for HIV-Infected Patients. In: Kazmierski, WM., editor. *Antiviral Drugs: From Basic Discovery Through Clinical Trials.* Wiley; New York: 2011. p. 31-45.
26. Kovalevsky AY, Liu F, Leshchenko S, Ghosh AK, Louis JM, Harrison RW, Weber IT. Ultra-high Resolution Crystal Structure of HIV-1 Protease Mutant Reveals Two Binding Sites for Clinical Inhibitor TMC114. *J. Mol. Biol.* 2006; 363:161–173. [PubMed: 16962136]
27. Ghosh AK, Chapsal BD, Baldrige A, Steffey MP, Walters DE, Koh Y, Amano M, Mitsuya H. Design and Synthesis of Potent HIV-1 Protease Inhibitors Incorporating Hexahydrofuropranol-Derived High Affinity P₂ Ligands: Structure – Acitivity Studies and Biological Evaluation. *J. Med. Chem.* 2011; 54:622–634. [PubMed: 21194227]
28. Ali R, Siddiqui N. Biological Aspects of Emerging Benzothiazoles: a Short Review. *J. Chem.* 2013:1–12.
29. Seth S. A Comprehensive Review on Recent Advances in Synthesis and Pharmacotherapeutic Potential of Benzothiazoles. *Antiinflamm. Antiallergy Agents Med. Chem.* 2015; 14:98–112. [PubMed: 26017385]
30. Mukherjee S, Corey EJ. [4 + 2] Cycloaddition Reactions Catalyzed by a Chiral Oxazaborolidinium Cation. Reaction Rates and Diastereo-, Regio-, and Enantioselectivity Depend on Whether Both Bonds are Formed Simultaneously. *Org. Lett.* 2010; 12:1024–1027. [PubMed: 20131879]
31. Reddy KM, Bhimireddy E, Thirupathi B, Breitler S, Yu S, Corey EJ. Cationic Chiral Fluorinated Oxazaborolidines. More Potent, Second-Generation Catalysts for Highly Enantioselective Cycloaddition Reactions. *J. Am. Chem. Soc.* 2016; 138:2443–2453. [PubMed: 26812167]
32. Lee J-E, Kwon J, Yun J. Copper-Catalyzed Addition of Diboron Reagents to α,β -Acetylenic Esters: Efficient Synthesis of β -Boryl- α,β -Ethylenic Esters. *Chem. Commun.* 2008; 6:733–734.
33. Nicolaou KC, Adsool VA, Hale CRH. An Expedient Procedure for the Oxidative Cleavage of Olefinic Bonds with $\text{PhI}(\text{OAc})_2$, NMO, and Catalytic OsO_4 . *Org. Lett.* 2010; 12:1552–1555. [PubMed: 20192259]
34. Ghosh AK, Chapsal BD, Baldrige A, Ide K, Koh Y, Mitsuya H. Design and Synthesis of Stereochemically Defined Novel Spirocyclic P₂-Ligands for HIV-1 Protease Inhibitors. *Org. Lett.* 2008; 10:5135–5138. [PubMed: 18928291]
35. Ghosh AK, Chapsal BD, Parham GL, Steffey M, Agniswamy J, Wang Y-F, Amano M, Weber IT, Mitsuya H. Design of HIV-1 Protease Inhibitors with C3-Substituted Hexahydrocyclopentafuranyl Urethanes as P₂-Ligands: Synthesis, Biological Evaluation, and Protein–Ligand X-ray Crystal Structure. *J. Med. Chem.* 2011; 54:5890–5901. [PubMed: 21800876]

36. Katsuki T, Sharpless KB. The First Practical Method for Asymmetric Epoxidation. *J. Am. Chem. Soc.* 1980; 102:5974–5976.
37. Gao Y, Hanson RM, Klunder JM, Ko SY, Masamue H, Sharpless KB. Catalytic Asymmetric Epoxidation and Kinetic Resolution: Modified Procedures Including In Situ Derivatization. *J. Am. Chem. Soc.* 1987; 109:5765–5780.
38. Ghosh AK, Schiltz GE, Rusere LN, Osswald HL, Walters DE, Amano M, Mitsuya H. Design and Synthesis of Potent Macrocyclic HIV-1 Protease Inhibitors Involving P1–P2 Ligands. *Org. Biomol. Chem.* 2014; 12:6842–6854. [PubMed: 25050776]
39. Gololobov YG, Zhmurova IN, Kasukhin LF. Sixty Years of Staudinger Reaction. *Tetrahedron.* 1981; 37:437–472.
40. Toth MV, Marshall GR. A Simple, Continuous Fluorometric Assay for HIV Protease. *Int. J. Pept. Protein Res.* 1990; 36:544–550. [PubMed: 2090647]
41. Koh Y, Amano M, Towata T, Danish M, Leshchenko-Yashchuk S, Das D, Nakayama M, Tojo Y, Ghosh AK, Mitsuya H. *In Vitro* Selection of Highly Darunavir-Resistant and Replication-Competent HIV-1 Variants by Using a Mixture of Clinical HIV-1 Isolates Resistant to Multiple Conventional Protease Inhibitors. *J. Virol.* 2010; 84:11961–11969. [PubMed: 20810732]
42. Hughes PJ, Cretton-Scott E, Teague A, Wensel TM. Protease Inhibitors for Patients with HIV-1 Infection: A Comparative Overview. *Pharm. Therap.* 2011; 36:332–345.
43. Amano M, Koh Y, Das D, Li J, Leschenko S, Wang YF, Boross PI, Weber IT, Ghosh AK, Mitsuya H. A Novel Bis-Tetrahydrofuranylurethane-Containing Nonpeptidic Protease Inhibitor (PI), GRL-98065, is Potent Against Multiple-PI-Resistant Human Immunodeficiency Virus In Vitro. *Antimicrob. Agents Chemother.* 2007; 51:2143–2155. [PubMed: 17371811]
44. Koh Y, Das D, Leschenko S, Nakata H, Ogata-Aoki H, Amano M, Nakayama M, Ghosh AK, Mitsuya H. GRL-02031, a Novel Nonpeptidic Protease Inhibitor (PI) Containing a Stereochemically Defined Fused Cyclopentanyltetrahydrofuran Potent Against Multi-PI-Resistant Human Immunodeficiency Virus Type 1 In Vitro. *Antimicrob. Agents Chemother.* 2009; 53:997–1006. [PubMed: 18955518]
45. For details of X-ray studies, please see Supporting Information.

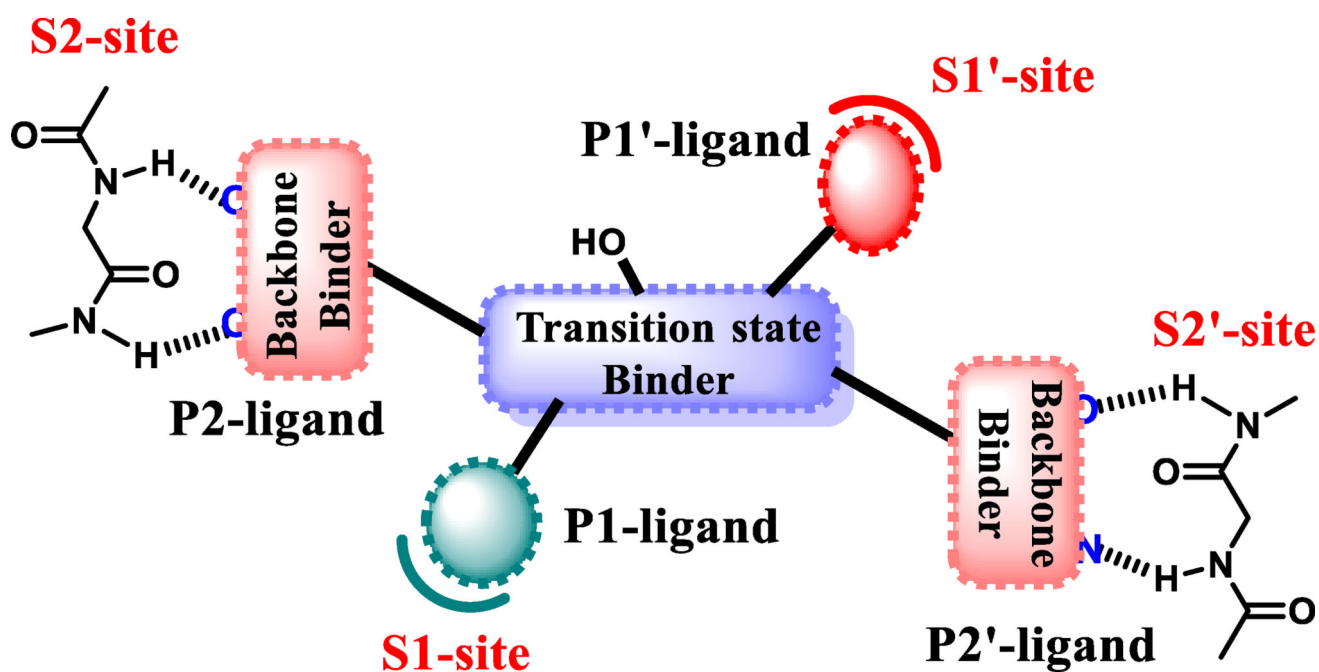


Figure 1. Proposed model for the design of PIs to combat drug resistance. The model suggests the formation of robust hydrogen bonds by the P2- and P2'-ligands simultaneously in both the S2 and S2'-subsites. The transition-state hydroxyl group binds to catalytic aspartates and the P1 and P1'-ligands fill in the S1 and S1'-subsites.

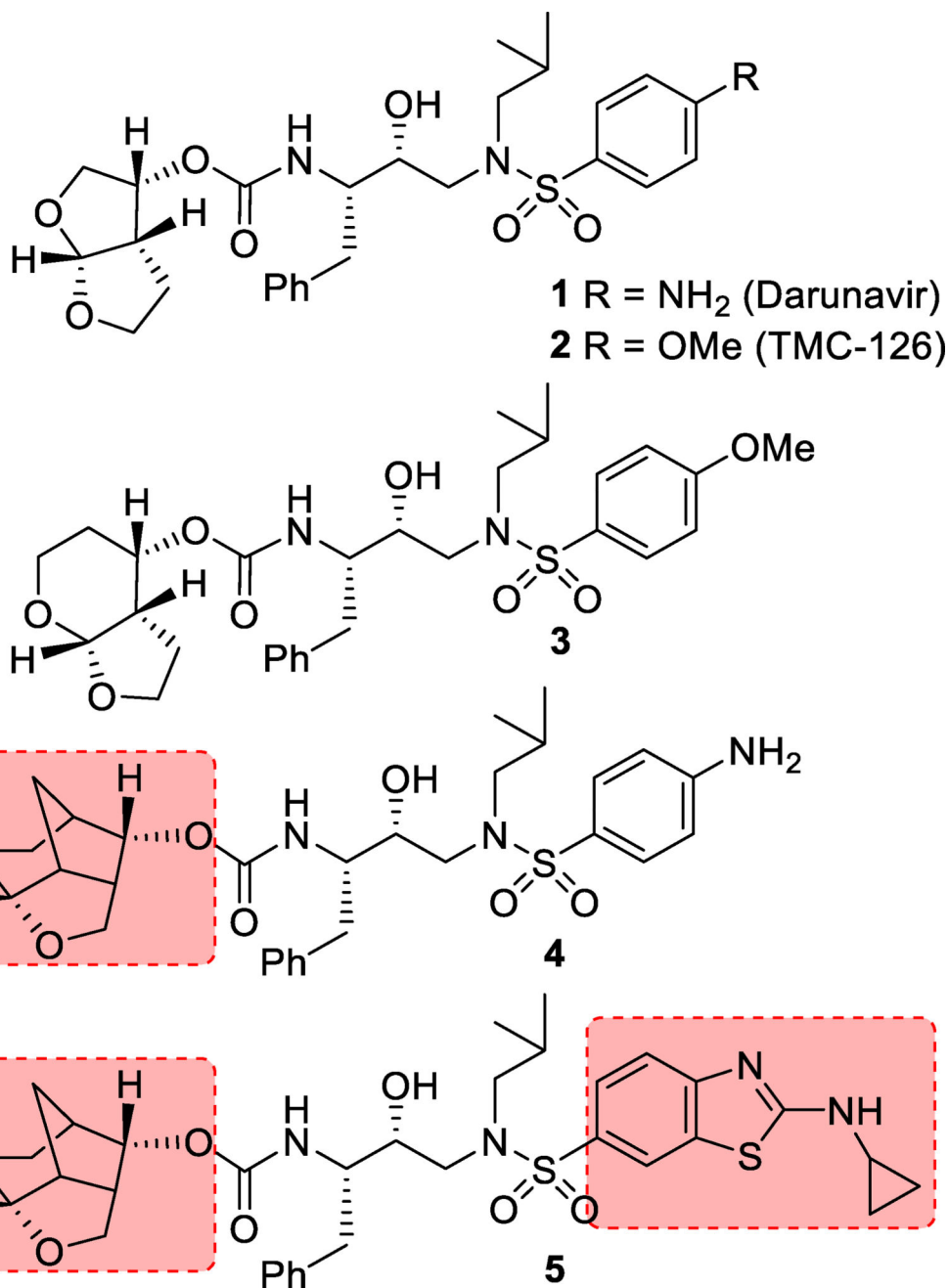


Figure 2.
Structures of HIV-1 protease inhibitors

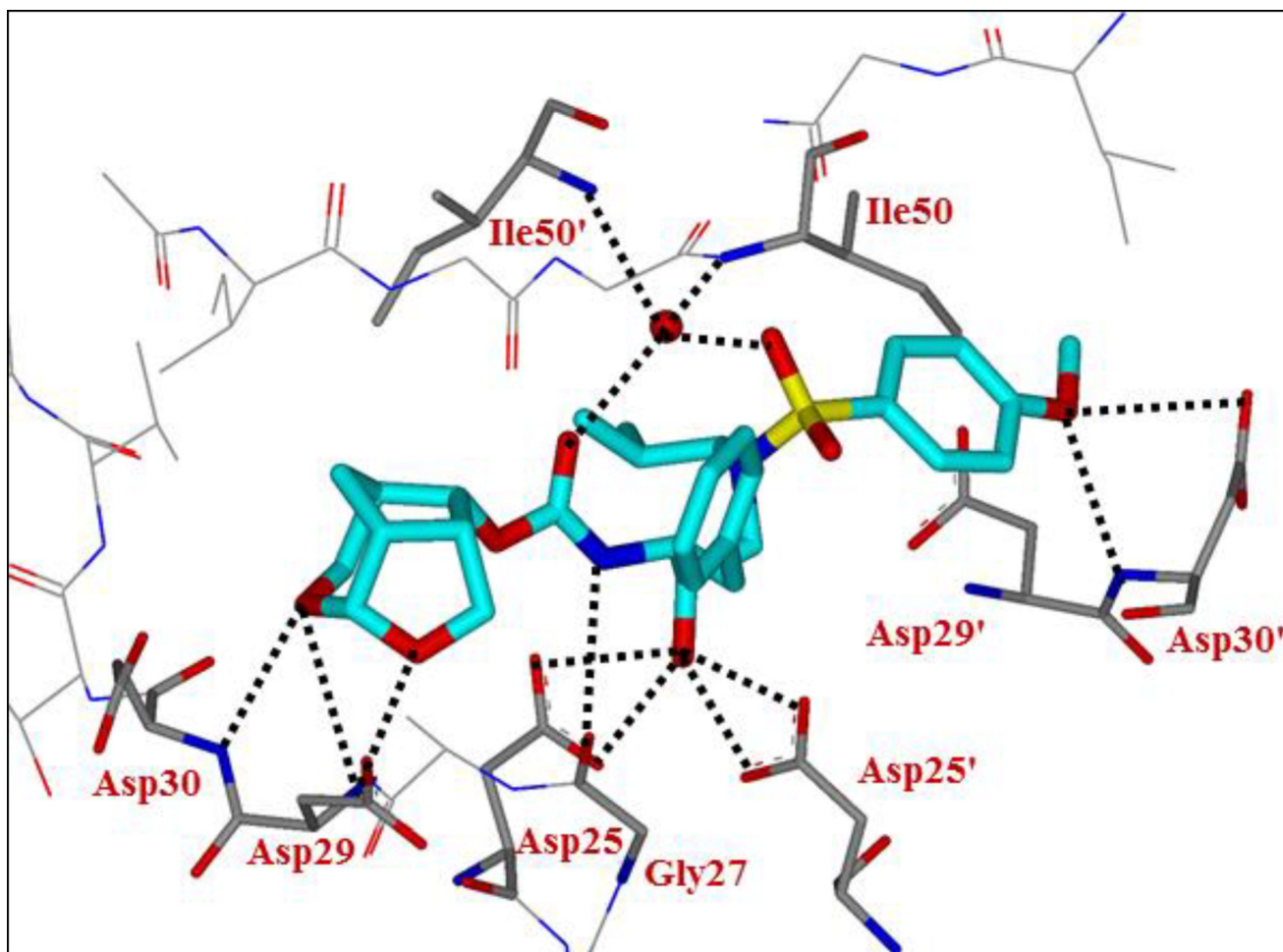


Figure 3. Inhibitor **25**-bound X-ray structure of HIV-1 protease (PDB code: 5ULT). The major orientation of the inhibitor is shown. The inhibitor carbon atoms are shown in cyan, water molecules are red spheres, and the hydrogen bonds are indicated by dotted lines.

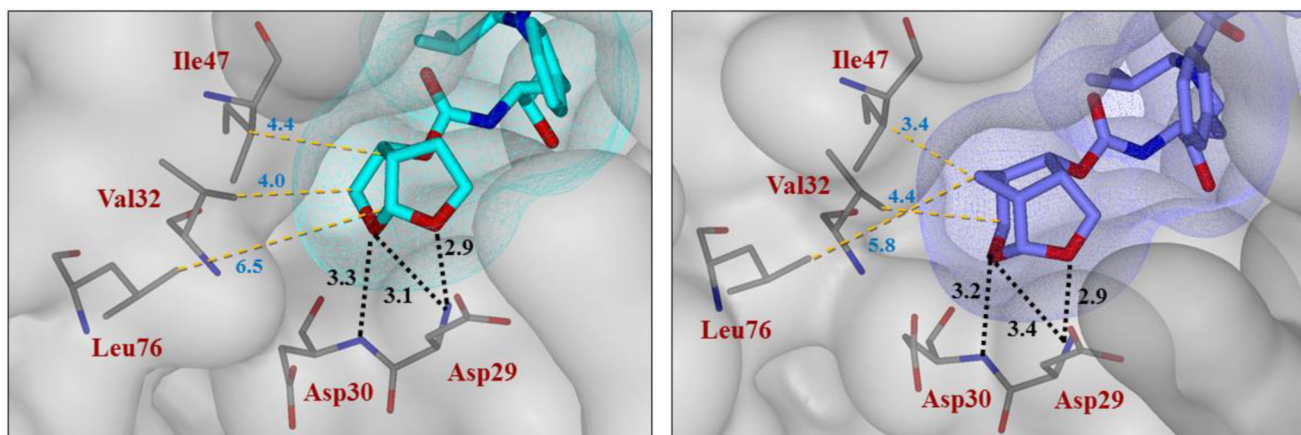


Figure 4. Side by side comparison of binding properties of P2 *bis*-THF moiety in darunavir-bound HIV-1 protease (left, cyan), X-ray structure (PDB code: 2IEN) with the P2 *crn*-THF moiety of inhibitor **25**-bound HIV-1 protease (right, purple), X-ray structure (PDB code: 5ULT) inside the S2 subpocket. Both groups are located close to the periphery of the protease active site and form three hydrogen bonds in a similar fashion (black dashes). The *crn*-THF is bulkier with extended triangle-shaped surface pointing towards the hydrophobic region consisting of Ile47, Val32 and Leu76. The *crn*-THF forms closer van der Waals interactions with Ile47 compared to the *bis*-THF.

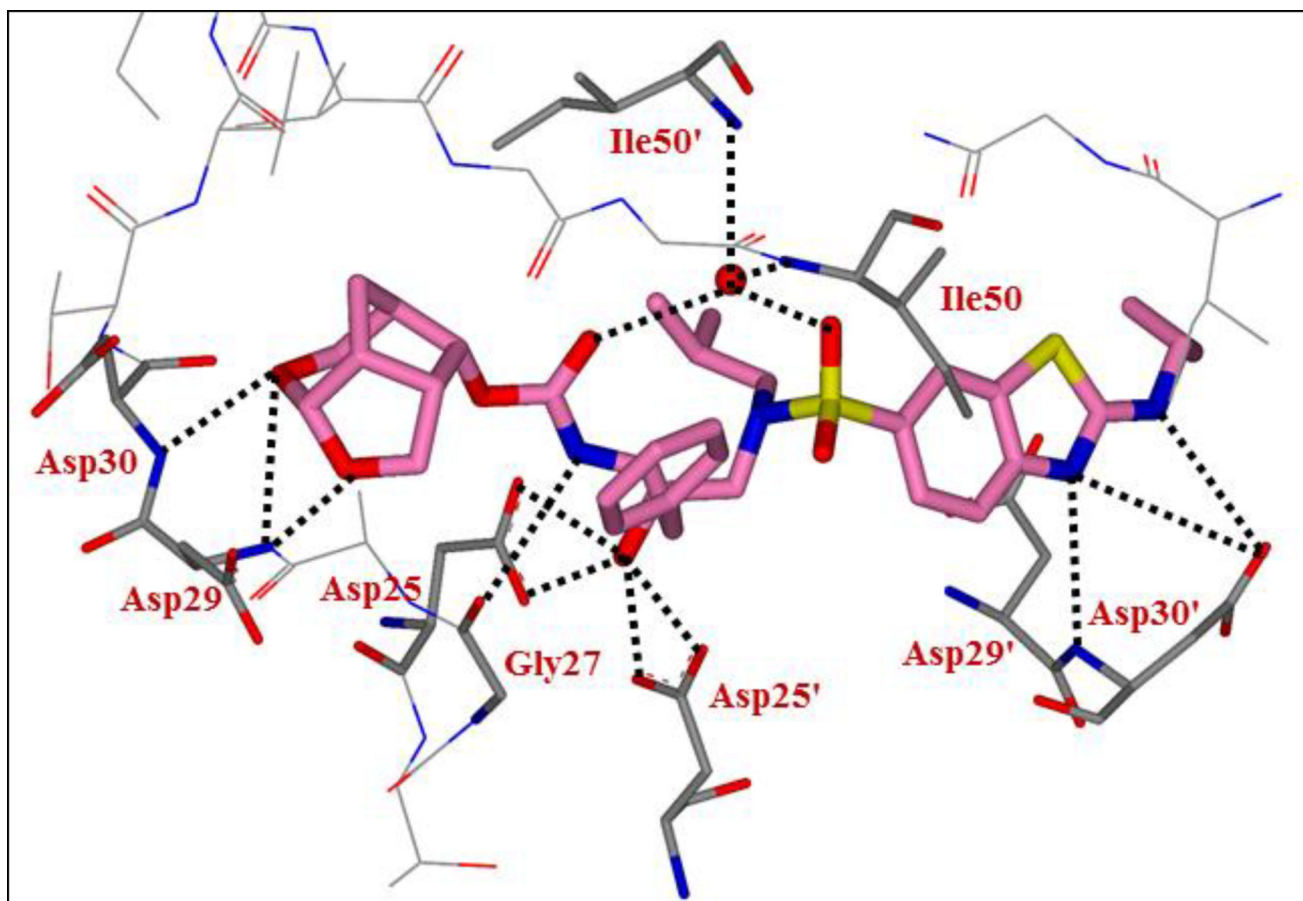


Figure 5. Inhibitor **5**-bound HIV-1 protease X-ray structure is shown (PDB code: 5TYR). The inhibitor carbon atoms are shown in magenta and hydrogen bonds are shown by dotted lines.

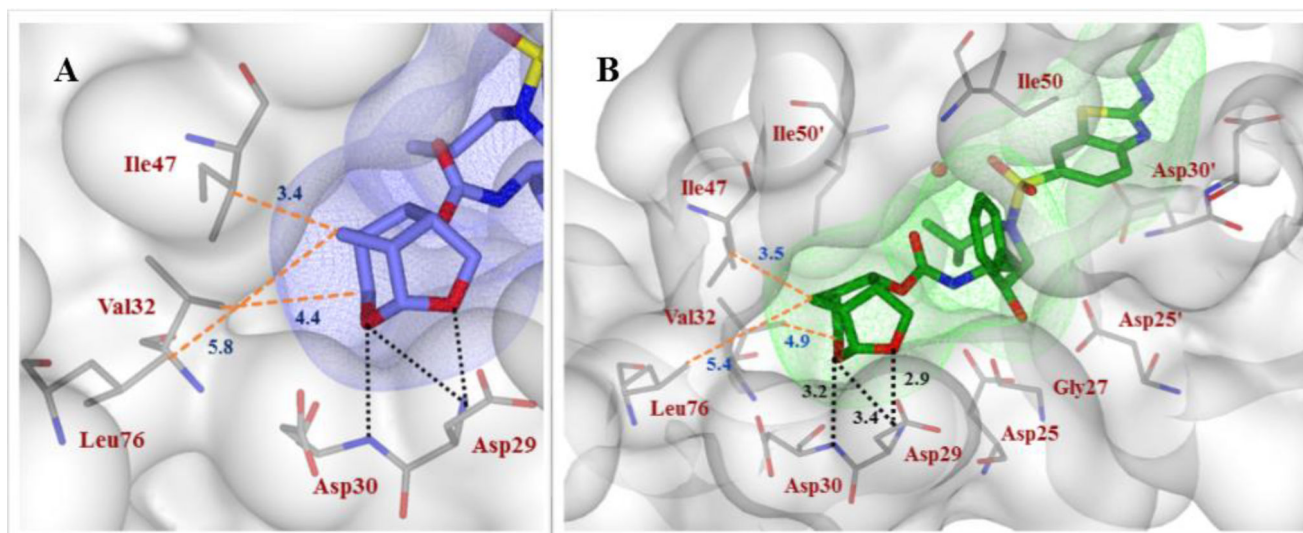
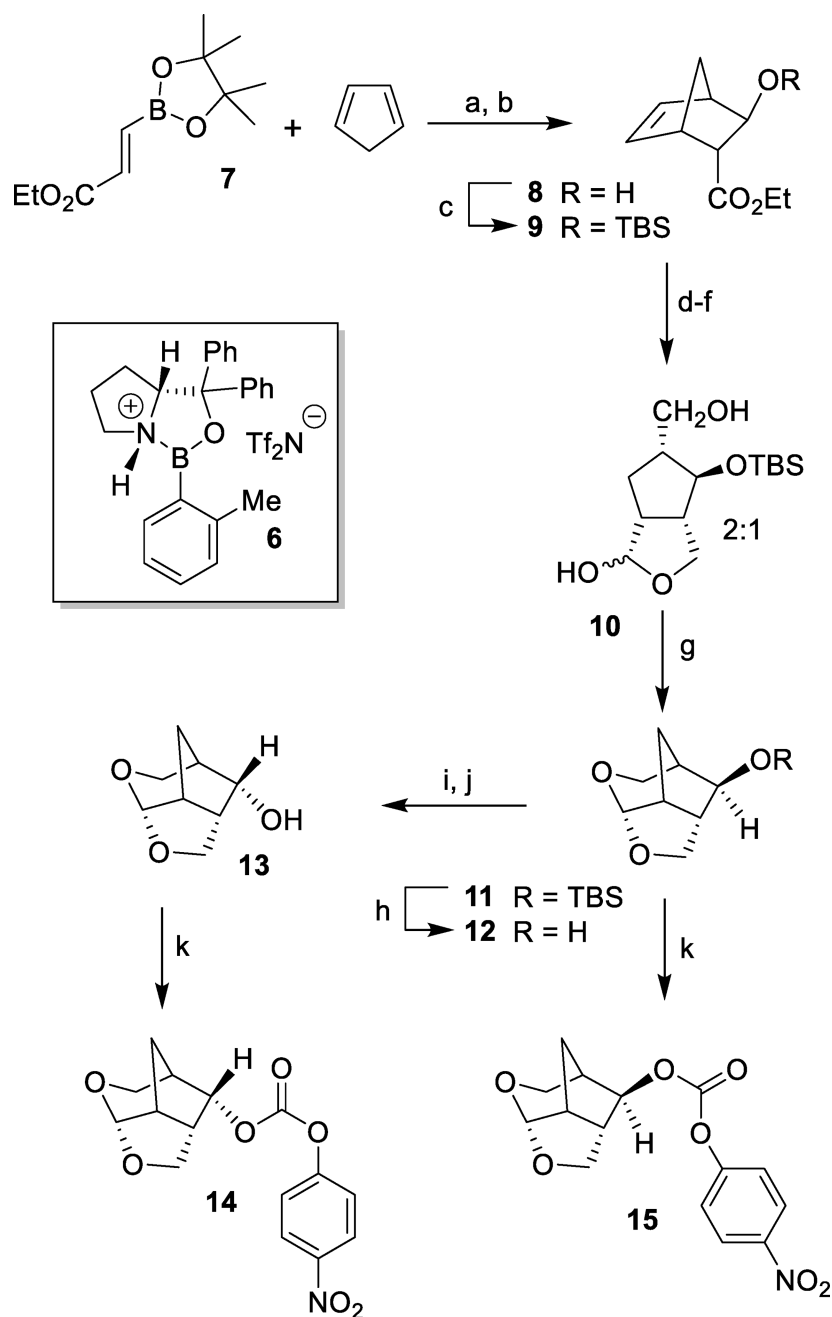
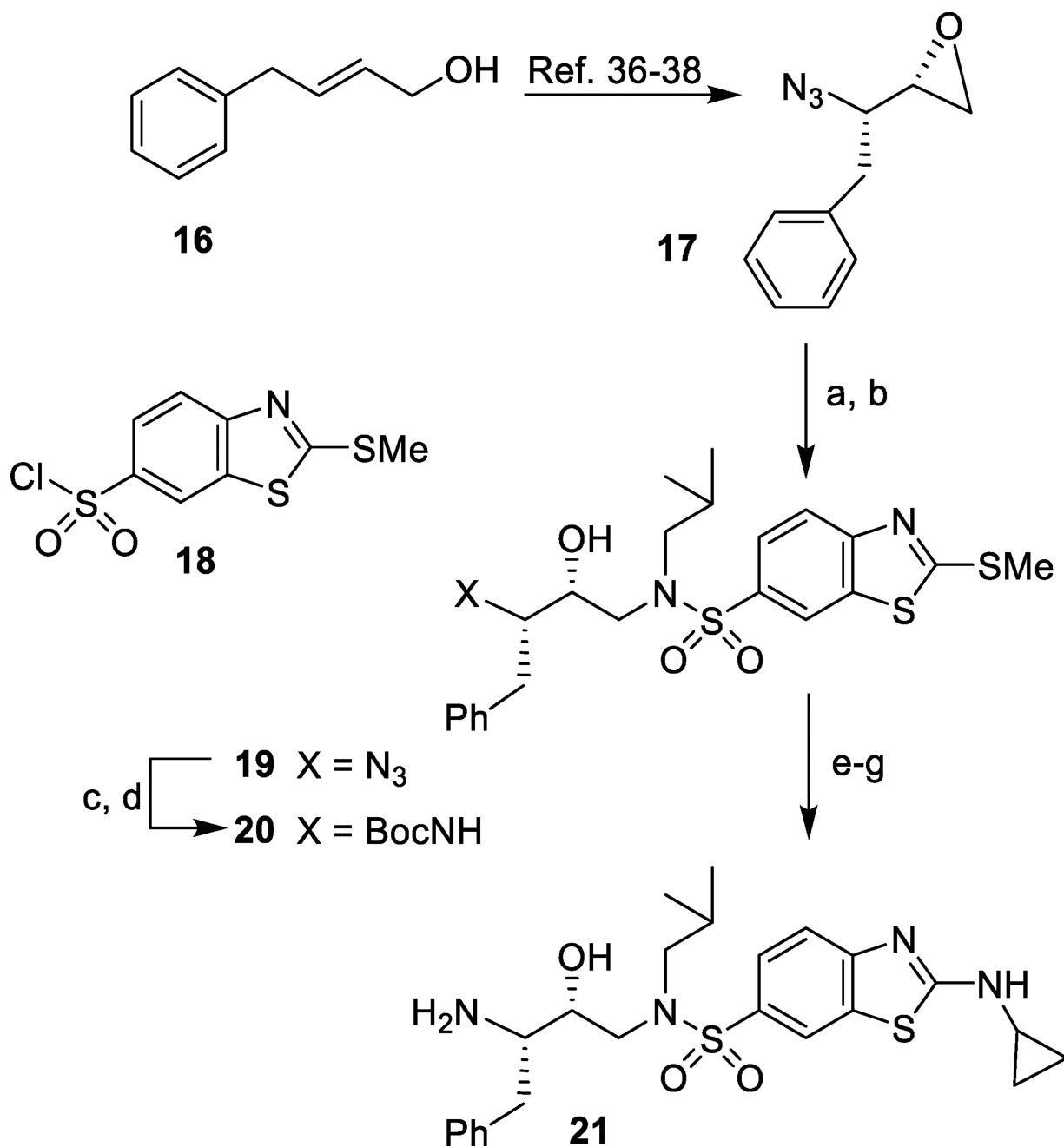


Figure 6. Comparison of the binding properties of the P2 *crn*-THF moiety of inhibitor **25**-bound HIV-1 protease (panel **A**, purple), X-ray structure (PDB code: 5ULT) and inhibitor **5**-bound HIV-1 protease (panel **B**, green), X-ray structure (PDB code: 5TYR) inside the S2 subpocket. The hydrogen bonds with the backbone atoms are shown in black dashes. The *crn*-THF in both inhibitors **5** and **25** form closer van der Waals interactions.

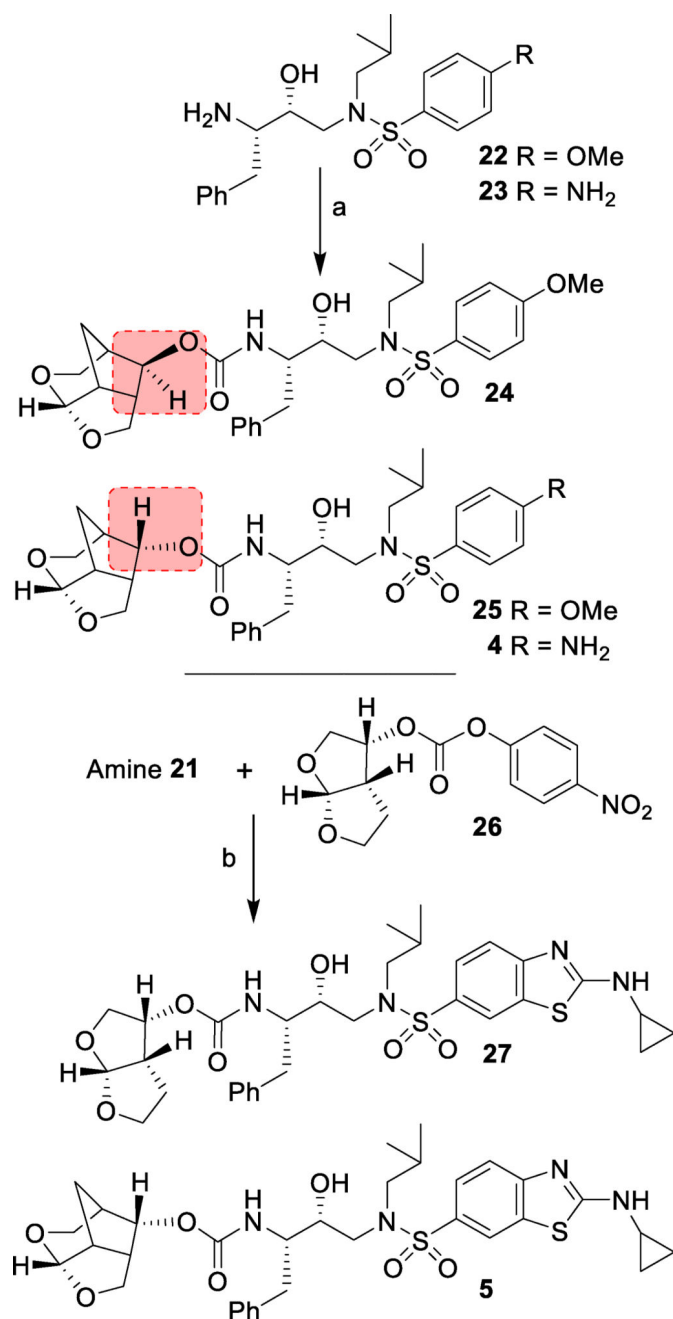


Scheme 1.

Synthesis of *crn*-THF ligand **13**. Reagents and chemicals. (a) **6** (20 mol%), CH₂Cl₂, -78 °C; (b) KHCO₃, H₂O₂, 0 °C, (80% for 2 steps); (c) TBSOTf, 2,6-lutidine, 0 °C to 23 °C, CH₂Cl₂, (95%); (d) LAH, THF, 0 °C to 23 °C; (e) OsO₄, NMO, 23 °C, acetone:H₂O (10:1); then PhI(OAc)₂, 23 °C; (f), DIBAL-H, CH₂Cl₂, 0 °C, (62% for 3 steps); (g) TFA, CH₂Cl₂, 0 °C, (74%); (h) TBAF, THF, 0 °C to 23 °C; (i) Dess-Martin Periodinane, Na₂HPO₄, CH₂Cl₂, 0 °C to 23 °C; (j) NaBH₄, MeOH, 0 °C, (70% for 3-steps); (k) 4-NO₂-PhOCOCl, pyridine, CH₂Cl₂, 0 °C to 23 °C, (83–95%).

**Scheme 2.**

Synthesis of sulfonamide isostere **21**. Reagents and chemicals. (a) *i*-BuNH₂, *i*-PrOH, 65 °C; (b) **18**, CH₂Cl₂, Et₃N, 23 °C, (90% over 2-steps); (c) Ph₃P, THF-H₂O (3:1), 23 °C; (d) Boc₂O, THF-H₂O (1:1), NaHCO₃, 23 °C, (85% over 2-steps); (e) *m*-CPBA, CH₂Cl₂, 23 °C; (f) cyclopropylamine, THF, 65 °C, (91% over 2-steps); (g) TFA, CH₂Cl₂, 0 °C (99%).

**Scheme 3.**

Synthesis of PIs. Reagents and chemicals. (a) carbonate **14** or **15**, DIPEA, CH₃CN, 23 °C; (b) amine **21** and carbonate **26** or **14**, DIPEA, CH₃CN, 23 °C, (50–60%).

Table 1

Enzymatic inhibitory and antiviral activity of inhibitors

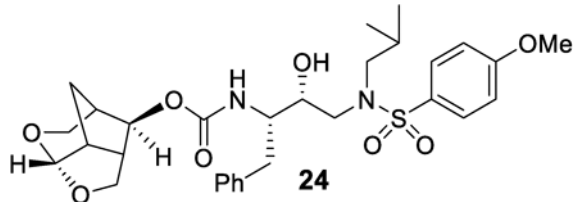
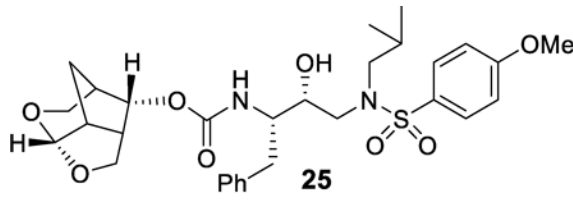
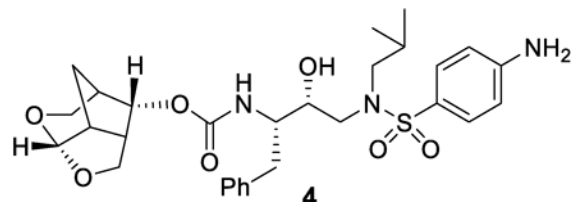
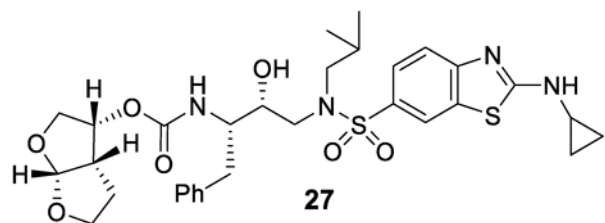
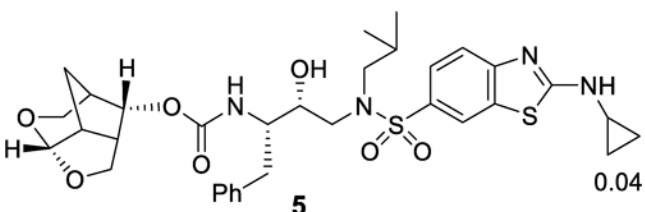
Entry	Inhibitor	K_i (nM)	IC_{50} (nM)
1.	 24	10.8	>1000
2.	 25	0.014	2.7
3.	 4	0.013	2.8
4.	 27	0.01	1.9
5.	 5	0.04	0.26

Table 2
Antiviral activity of novel three compounds against highly DRV-resistant HIV-1 variants.

	Mean IC ₅₀ in nM ± SD (fold-change) ^{a,b}				
	LPV	DRV	4	27	5
HIV-1 _{INL4-3}	20 ± 4	3.8 ± 0.7	3.3 ± 1.2	2.0 ± 0.8	0.39 ± 0.06
HIV-1 _{DRV^RP20}	>1,000 (>50)	34 ± 19 (9)	30 ± 10 (9)	7.7 ± 2 (4)	0.17 ± 0.01 (0.4)
HIV-1 _{DRV^RP30}	>1,000 (>50)	360 ± 10 (95)	340 ± 18 (103)	30 ± 5 (15)	1.8 ± 0.5 (5)
HIV-1 _{DRV^RP51}	>1,000 (>50)	3,200 ± 300 (842)	>1,000 (>303)	480 ± 83 (240)	35 ± 12 (90)

^a MT-4 cells (1×10^4) were exposed to 50 TCID₅₀S of wild-type HIV-1_{INL4-3}, HIV-1_{DRV^RP20}, HIV-1_{DRV^RP30}, or HIV-1_{DRV^RP51} and cultured in the presence of various concentrations of each PI, and the IC₅₀ values were determined using the p24 assay. The amino acid substitutions identified in protease of HIV-1_{DRV^RP20}, HIV-1_{DRV^RP30}, and HIV-1_{DRV^RP51} compared to HIV-1_{INL4-3} include L101/I15V/K20R/L24I/V32I/M36I/M46L/L63P/V82A/L89M; L101/I15V/K20R/L24I/V32I/M36I/M46L/L63P/K70R/V82A/I84V/L89M and L101/I15V/K20R/L24I/V32I/L33F/M36I/M46L/I54M/L63P/K70Q/V82I/I84V/L89M, respectively.

^b All assays were conducted in triplicate, and the data shown represent mean values (± 1 standard deviation) derived from the results of three independent experiments.

Table 3

Antiviral activity of inhibitor **5** against highly PI-resistant HIV-1 variants.

Virus species	Mean IC ₅₀ in nM ± SD (fold-change)				
	LPV	ATV	DRV	5	
Wild-type	20 ± 4	4.2 ± 0.7	3.8 ± 0.7	0.39 ± 0.06	
HIV-1 _{PI} ^R *					
HIV-1 _{NI4-3}	>1,000 (>50)	510 ± 14 (121)	45 ± 2 (12)	0.03 ± 0.01 (0.08)	
HIV-1 _{APV-5µM}	310 ± 18 (16)	3.8 ± 2.5 (0.9)	25 ± 21 (7)	0.27 ± 0.1 (0.7)	
HIV-1 _{LPV-5µM}	>1,000 (>50)	45 ± 19 (11)	430 ± 40 (113)	0.0026 ± 0.0006 (0.007)	
HIV-1 _{IDV-5µM}	170 ± 20 (9)	62 ± 10 (15)	30 ± 17 (8)	0.012 ± 0.013 (0.03)	
HIV-1 _{NFV-5µM}	42 ± 7 (2)	17 ± 3 (4)	8.2 ± 3.8 (2)	0.028 ± 0.02 (0.07)	
HIV-1 _{ATV-5µM}	330 ± 30 (17)	>1,000 (>238)	36 ± 3 (9)	0.19 ± 0.06 (0.5)	
HIV-1 _{TPV-15µM}	>1,000 (>50)	>1,000 (>238)	39 ± 5 (10)	0.057 ± 0.03 (0.15)	

* *In vitro* PI-selected HIV-1 variants. The amino acid substitutions identified in protease of HIV-1_{SQV-5µM}, HIV-1_{APV-5µM}, HIV-1_{LPV-5µM}, HIV-1_{IDV-5µM}, HIV-1_{NFV-5µM}, HIV-1_{ATV-5µM}, and HIV-1_{TPV-15µM} compared to the wild-type HIV-1_{NI4-3} include L101I/N37D/G48V/I54V/L63P/G73C/I84V/L90M, L101F/V32I/M46I/I54M/A71V, L101F/V32I/M46I/I47A/A71V/I84V, L101F/L24I/M46I/I54V/L63P/A71V/G73S/V82T, L101F/K20T/D30N/K45I/A71V/V77I, L23I/E34Q/K43I/M46I/I50L/G51A/L63P/A71V/V82A/T91A, and L101/L33I/M36I/M46I/I54V/K55R/I62V/L63P/A71V/G73S/V82T/L90M/I93L, respectively. Numbers in parentheses represent fold changes in IC₅₀s for each isolate compared to the IC₅₀s for wild-type HIV-1_{NI4-3}. All assays were conducted in triplicate, and the data shown represent mean values (± 1 standard deviation) derived from the results of three independent experiments.